GRAPHENE SUPPLEMENTED MICROBUBBLE FLOTATION FOR HEAVY CRUDE OIL REMOVAL FROM CONTAMINATED SAND

IAN DARYL STA MARIA

Supervisor: Dr. Lau Ee Von

A Thesis
submitted in partial fulfillment of the requirements for the
Degree in Masters of Engineering (Mechanical)
Faculty of Engineering
Monash University

October 2018

Abstract

Oil spills are a major environmental concern around the world and much effort has gone into addressing this issue. It is crucial to remove and recover oil from sand contaminated by oil spills in order to return the environment to its natural state. Therefore, this research aims to investigate the oil recovery efficiency of microbubble flotation oil recovery method enhanced with dispersed graphene nanoparticle powder.

A preliminary study on the graphene-microbubble attachment was conducted by zeta potential measurements. It was determined that while both are negatively charged, the zeta potential measurements of graphene and microbubble were small in magnitude at pH 6 to 7 indicating instability thus attachment was still possible. The magnitude of zeta potential began increasing exponentially after pH 7 causing graphene-microbubble attachment to be more difficult. Derjaguin-Landau-Verwey-Overbeek (DLVO) theory was implemented to quantitatively display the inter particle forces between graphene and microbubble.
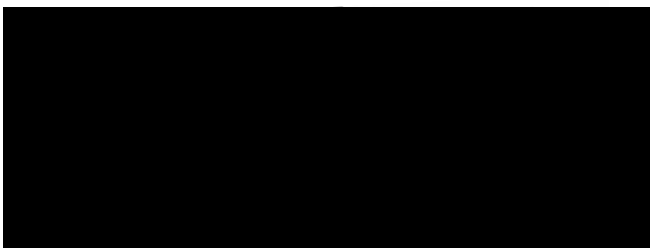
Characterization of GNP dispersions was also conducted in terms of density, interfacial tension, viscosity and pH. It was determined that the increase in GNP concentration up to 0.1 wt% would impact the density and interfacial tension of graphene/water dispersion while effects on viscosity and pH were negligibly small.

Oil recovery efficiency was investigated in terms of pH level, GNP concentration and temperature. Microbubble generation for oil flotation was done using a venturi tube. Results were on par with zeta potential measurements and the oil recovery rate was found to be 24.32% at pH 7, albeit a slightly higher recovery rate could be achieved due to the increase in oil-sand separation under alkaline conditions. At neutral pH, oil recovery benefited from both interfacial tension reduction which enhances oil-sand separation, as graphene-coated microbubble. Above pH 7, oil recovery only is only due to reduction in interfacial tension. As for GNP concentration, the optimum concentration of graphene was at 0.1wt%, achieving an efficiency rating of 23.7% at pH 7 and room temperature. However, the highest register of oil recovery efficiency was 70% at 80 ℃ and pH 7. This proved to be the optimum conditions for graphene supplemented microbubble oil flotation. Although the overall efficiency was found to be low, this study shows that graphene supplementation could be a promising additive in enhancing oil recovery using the flotation technology.

Certificate of Originality

I hereby declare that this submission is my own work and to the best of my knowledge it contains no materials previously published or written by another person, nor material which to a substantial extent has been accepted for the award of any other degree or diploma at Monash University or any other educational institution, except where due acknowledgement is made in the thesis. Any contribution made to the research by others, with whom I have worked at Monash University or elsewhere is explicitly acknowledged in the thesis.

I also declare that the intellectual content of this thesis is the product of my own work, except to the extent that assistance from others in the project's design and conception or in style, presentation and linguistic expression is acknowledged.

…..   ..

(IAN DARYL STA MARIA)

Acknowledgement

I would like to express my deepest appreciation and most gracious gratitude to my supervisor Dr. Lau Ee Von, who offered continuous support, advice and encouragement throughout the course of this research. This research project would not be possible without support from Dr. Lau Ee Von.

I would also like to express my gratitude and thanks to PhD graduate Ms. Amber Lim, FYP students Mr. Woo Wai Kit, Mr. Pratapan Tangarajah and Mr. Alan Kong for their support during the course of this research. I would also like to thank lab technician Mr. Mohammand Nasrun, for his technical assistance with the laboratory equipment.

Last but not least, I would like to thank all the people for their help directly and indirectly in completing this project.

TABLE OF CONTENTS

Contents

LIST OF FIGURES

LIST OF TABLES

CHAPTER 1: INTRODUCTION

1.1   Background on oil spills

On April 20, 2010, the Deepwater Horizon drilling rig, owned by British Petrol (BP), located in the Gulf of Mexico, was rocked by a massive explosion. This incident caused 11 casualties and sent a massive amount of oil gushing into the water. By the time the well was sealed months later, about 5 million barrels of oil had spilled into the Gulf [1,2]. The rig capsized and sank two days later leaving behind a number of negative effects on the environment. This incident remains one of the largest oil spills to occur in recent times. Oil spills have remained a common occurrence and a major concern to everyone involved in the industry today. It was estimated that approximately 400 to 600 metric tons of crude oil, per year, are leaked or spilled into the water and polluting the environment [3]. The Deepwater Horizon incident was said to be one of the worst environmental disasters the United States have faced [4]. The disaster contaminated beaches and marshes between 633 to 1300 miles of the United States coastline around the Gulf of Mexico, causing many long-lasting effects on the ecosystem.

The oil spilled into the ocean eventually reached the shores and thus contaminating the rocks and soils. It has been reported that the oil deposited onto the sand could penetrate deep into the ground as far as 25cm depending on grain size [5]. Contamination and erosion of land have led to the death of most marsh vegetation and many life forms. A study indicated that the pollution caused a shift in the ecological food chain causing any species, like fungi, that benefit from the pollution to dominate and multiply exponentially; inducing harm onto the rest [1].The oil contamination also inhibits the structure of the sand foundation affecting the bearing capacity causing soil erosion and structural collapse [6]. Other such incident was during the

Gulf War, 1990 to 1991, which is still considered the largest oil spill in history. Iraqi forces attempted to prevent American soldiers from landing on their shores by opening valves at an offshore oil terminal and dumping oil into the ocean. This resulted in a thick 4-inch oil slick which spread across 4,000 square miles in the Persion gulf. The nearby regions, as well as the Kuwait dessert were affected by the massive oil spill where approximately 1.1 billion liters of crude oil were spilt [7].

1.2   Oil flotation remediation technology

Today, much effort has gone into researching various methods of oil remediation such as sand washing, thermal desorption, coal agglomeration, bioremediation, chemical oxidation and several others [8]. However, studies indicated that most methods are encumbered by mediocre success rates and high implementation costs [7].   One method of oil recovery that possesses great prospects is the flotation, remediation method. The flotation system can be described as a physiochemical method that uses gas bubbles to separate the hydrophilic from the hydrophobic material that is acted on due to dissimilarities in surface properties of both materials which are affected by numerous factors such as mechanical, chemical and physiochemical properties [9-11].

The objective of this method is to separate the oil particles from the sand thus allowing it to float to the surface and then be removed through water treatment and mineral recovery [12]. The premise of this process is to achieve oil-water-sand separation through agitation through methods such as electrolysis, introduction of mechanical agitation through air injection or any other processes [13]. Studies have shown that the amount of agitation through the introduction of bubbles at varying sizes has achieved positive oil recovery efficiency [14]. At present, the flotation technology have been seen capable of separating liquid from solids, such as in the removal of paraffin oil, crude oil as well as vegetable oil from soil [15-17].

1.3   Coating of bubbles

Coated bubbles have been vastly studied in many fields, particularly in medicinal and environmental applications. By coating bubbles, its mechanical and chemical properties can be manipulated to enhance its effectiveness. For example, a recent study investigated the egg white protein and bovine serum albumen coated bubbles for copper ion removal through the flotation method [18,19]. Furthermore, it has been report that the use of oil-coated bubbles can be successfully employed in flotation of minerals [20,21].

1.4   Graphene for oil adsorption

On another occasion, the discovery of graphene by Prof. Andre Geim and Prof. Kotsya Novoselov in 2004 boomed into the research field opening doors to many new ideas [22]. Much research has gone into the potential application of graphene due to its incredible physical, mechanical, electrical and chemical properties [23]. Graphene has a two-dimensional atomic structure with a honeycomb lattice arrangement that is a single atom thick [24] making it an attractive and intriguing material to experiment with. The simplicity of graphene also allows it to be assembled and shaped into many different formations resulting in a many possibilities of applications [24].

To date, much research has been done on graphene in terms of oil adsorption as it also has an exceptionally large exposed surface area and super-hydrophobic properties which have excellent potential in terms of oil adsorption [25]. Studies have shown that graphene-based sponges or gels have displayed great oil adsorption capabilities, along with high elasticity, porousness and recyclability [25,26]. Therefore, the discovery of graphene has displayed great potential to affect the efficiency of oil remediation technology and techniques.

1.5   Problem statement

At present, there are various methods developed and tested to remove oil from contaminated sand, using physical, chemical, biological and other means [1]. While each have their benefits, their disadvantages are also largely apparent. Physical removal methods employ thermal or combustion techniques which produce hazardous fumes which affects human safety, as well as the environment. The energy consumption of these methods are also very large and proportionate to the sand sample size thus incurring a large sum of operating costs [27,28]. Chemical methods employs solvents and/or additives dependant on various factors such as soil composition and type of contaminant. Depending on these factors, hazardous chemicals at high concentrations may be employed thus requiring expensive safety measures and a large amount of clean-up work to ensure no harm is done on living organisms and the surrounding environment [29]. Biological methods such as bioremediation require a larger amount of time compared to other methods. Furthermore, the addition of enzymes or bacteria to address the contaminant also could affect the ecosystem of the surrounding environment [30-32].

However, methods such as microbubble coating can increase the efficiency of oil remediation thus alleviating the burden of cost and energy consumption. Along with the discovery of a hydrophobic and high adsorption material such as graphene, it is possible to address the shortcomings of todays oil removal methods. Therefore, in order to increase the efficiency of oil removal from contaminated sand, this research employs the physical removal method of microbubble flotation method with the application of graphene-supplemented microbubble coating. As such, this research project aims to investigate the effects of graphene supplemented microbubbles for oil removal from oil-contaminated sand by characterizing its contributions to the flotation process and obtaining the optimum conditions for maximum efficiency of oil-sand separation.

1.6   Objectives

The main objective of this research project is to investigate the efficiency of graphene enhanced bubbles in the oil flotation remediation method via venturi tube generation. The specific aims of this research project are as listed below:

- To investigate the effects of pH on graphene-bubble attachment using zeta-potential measurements and DLVO theory.

- To characterize graphene nanoparticle powder (GNP) dispersions in terms of density, interfacial tension, viscosity, and pH.

- To investigate the oil removal efficiency of graphene supplemented flotation technology against pH, GNP concentration and temperature.

CHAPTER 2: LITERATURE REVIEW

2.1   Flotation technology

Oil spills affect not only the safety of life forms in seawater and shorelines but also damage the economics and socio-economics of the surrounding regions. If left untreated, it will further damage to affected environment and will only increase in severity through time, further complicating the removal and recovery process. Therefore it is vital that swift and efficient action be taken to address the incident as quick as possible. Many different solutions have been developed in the passing years which utilize physical and biological means to remove oil from contaminated sand. However, the issues of time consumption and hazardous side-effects still persist in methods employed today. This shows that there is a need to determine an efficient, effective, simple, and environment friendly method to separate oil from contaminated sand.

One of the solutions in works is the use of flotation technology. This process is a combination of chemical and physical applications which enables the separation of oil from soil via a gas-liquid-solid system, utilizing the difference in surface properties of contaminant and soil. The mechanism of flotation lies in the usage of a medium, bubbles most commonly used, to dislodge hydrophobic contaminant particles from submerged soil and transport them to the surface for removal. The efficiency of the flotation process is affected by numerous factors, mechanical and chemical. The fundamental mechanics of flotation can be explained in four steps; a) generation of gas bubbles for flotation of oil contaminant, (b) bubble collision with oil contaminant, (c) bubble attachment with oil contaminant, (d) formation of stable bubble-particle attachment followed by subsequent flotation [33]. The success of oil recovery is in the ability of hydrophobic particles to attach to bubbles and raised to the surface thus the

initial attachment of bubbles and particle is crucial. When they are in close range, an intervening liquid film is formed, preventing the attachment, governed by the hydrodynamics non-contact forces that exist between them [34].

Therefore, much research has gone into improving and perfecting this process. The nature of the hydrophobic interaction required both experimental and theoretical verification as the lack of a reliable model to describe the drainage process of this thin film between bubble and particle [35]. Therefore, much research has been put into the development of the flotation system.

2.1.1 Methods of flotation technology

There are many different methods to apply the flotation technology which has been investigated and reviewed by researchers. Each method has their advantages and disadvantages hence it is vital that proper analysis of the situation is conducted prior to selection.

One of the methods of flotation technology is dissolved air flotation (DAF), where pressurized water is saturated with air and injected into a tank and with the release of pressure, through a relief valve, generates small air bubbles to float contaminants to the top [36-39]. This method has a high loading rate and produces quick results but suffer from high energy consumption, equipment complexity, cost and size. It is also capable of producing bubbles smaller than $10 \mu m$. This method is mostly employed in bitumen extraction [40,41].

Besides that, induced air flotation (IAF) is another method of flotation. The wastewater is saturated with air either directly in an aeration tank or induced through a pump or venture tube [42-44]. While this method is simplistic and energy consumption friendly, the inability bubble size small than mm range is a major drawback thus the DAF method is generally considered to be more effective than IAF [45,46].

Another method of flotation employed is the electro-flotation (EF) method, where electrolysis of diluted aqueous solution is used to produce gas bubbles at the electrode

for floating contaminants. This method has shown high removal efficiencies largely due to its production and uniform dispersal of extremely fine gas bubbles. However, this method suffers from low throughput due to rate of bubble emissions, as well as high long-term costs due to the depletion of electrodes **[47]**.

Centrifugal flotation (CF) is another commonly used method of flotation. This method is done by injecting air through a poruous wall in the aeration tank and is sheared into bubbles by high-velocity whirl flow generated by mechanical agitation or pump **[48,49]**. This method benefits from high loading rate but starts to lack efficiency as the size increases. Due to the agitation in the tank, the bubbles generated do not last long enough for a high recovery rate**[50-52]**.

Lastly, column flotation is a method commonly used for oily wastewater treatment and particle separation. This method works by injecting air through a sparger located at the bottom of the column to generate bubbles while the contaminant is fed through an entrance at the top. This allows the bubbles to intersect with the sinking contaminant as it rises thus providing a high probability of bubble-particle collision hence a higher recovery efficiency. However, this method suffer from low throughput as over-flooding of contaminants will cause the bubbles to over-attach with hydrophobic particles and thus break before floating to the surface **[53-56].**

2.1.2 Flotation technology in oil remediation

To date, flotation technology had been extensively researched for various applications such as paper deinking **[57]**, mineral processing **[58]**, and industrial wastewater treatment **[59]**. One area where flotation has shown great promise is in oil remediation for removal of inorganic and organic particles from contaminated soil. Therefore, much research has gravitated to further understanding this mechanism, and the development of technologies to achieve the best possible oil recovery rate.

2.1.3.1 Surfactant, foam and microfoams

Early studies began with the manipulation of temperature, as usage of hot water during the flotation process caused the oil density and interfacial tension to drop and allow for better separation. Other properties such as alkalinity and acidity were also investigated to optimum charge for better oil separation **[60]**.

Further studies then brought focus to the use of surfactants. *Surfactants* are compounds that lower the surface tension between two liquids, between a gas and a liquid, or between a liquid and a solid and it is known to increase contaminant solubility in the water phase. However, remediation with surfactants requires a great consumption of surfactant with low oil removal efficiency **[61-63]**. Furthermore, the cost and effort sand and surface decontamination proved an issue **[64]**. To improve the efficiency of surfactant use, soil texture and composition will have a different effect when flooded with different surfactants. Also, to achieve better efficiency, it is best to match specific surfactants to specific contaminant **[63]**. Several studies indicated that negative ionization of surfactants solutions produced better efficiencies due to the acidity of contaminants such as crude oil **[65,66]**.

The use of foams was also investigated as method of improving contact between surfactant and soil, as well as reducing the interfacial tension between the contaminant and the aqueous phase **[67,68]**. In addition, foams serve as carriers to transport contaminants, a similar method used to carry nutrients and oxygen in bioremediation processes **[69][70].** A laboratory study by Huang and Chang (2000) indicated that with foaming of surfactant at a 10/1 gas-liquid ratio, a 48% increase in oil removal efficiency was obtained as seen in **Figure 1**[**67**].
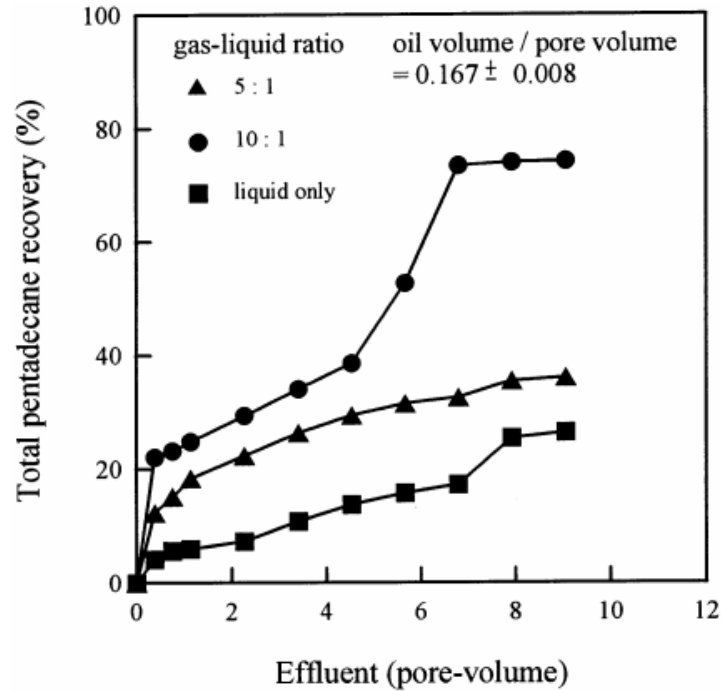
Figure 1 Total pentadecane recovery against Effluent at different gas-liquid ratio [67]

With the success of foams, focus then turned to the use of micro-foams, defined as colloidal gas aphrons (CGA) comprised of microbubbles. This was initially done by submitting the surfactant solution to high speed stirring of 5000 rpm or more to generate microbubbles of sizes between 10 to 100 μm **[71,72]**. The use of microfoams in surfactant flooding also caused smaller pressure drops thus relieving stress on pressure pumps without sacrificing efficiency **[73]**.

A study comparing the application surfactant solutions, foam and aphrons was conducted by Couto et al (2009) in an investigation on the remediation of sandy soils contaminated with diesel oil. It was determined that micro-foams attained the highest oil recovery efficiency of 96%, followed by regular foams 88% and lastly surfactant solutions of 35% only, as shown in **Figure 2**.
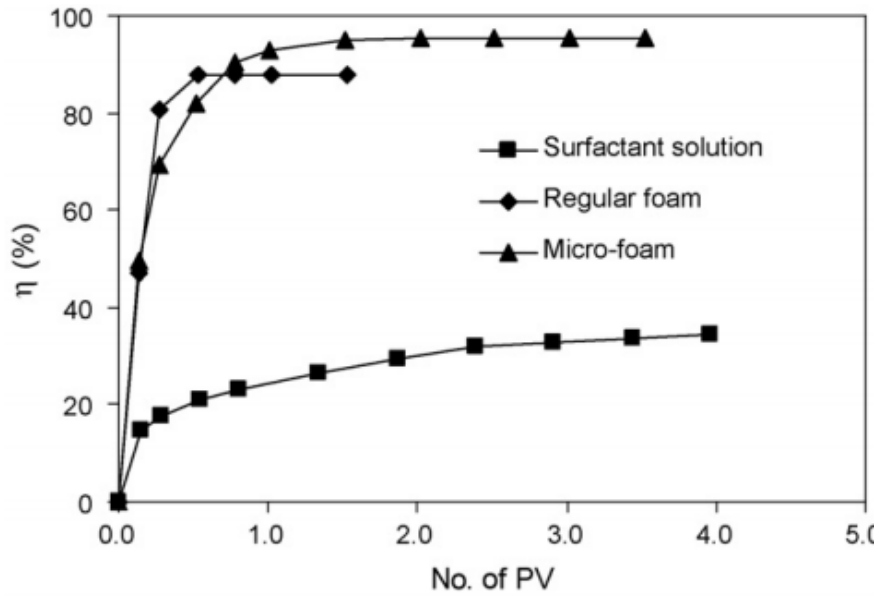
Figure 2 Recovery efficiency against Surfactant, Foam, Microfoam volume [74]

2.1.3.2 Additives

One other method of improving oil removal performance is the addition of chemical additives to the separation process during the preparation phase. The application of chemical additives proved to have benefited both the separating process, but also the removal process after flotation **[75-77]**. Additives could also be used as an oil agglomerate to enhance particle-bubble attachment **[78]**. **Figure 3** displays a diagram of agglomerate application for increasing attachment.
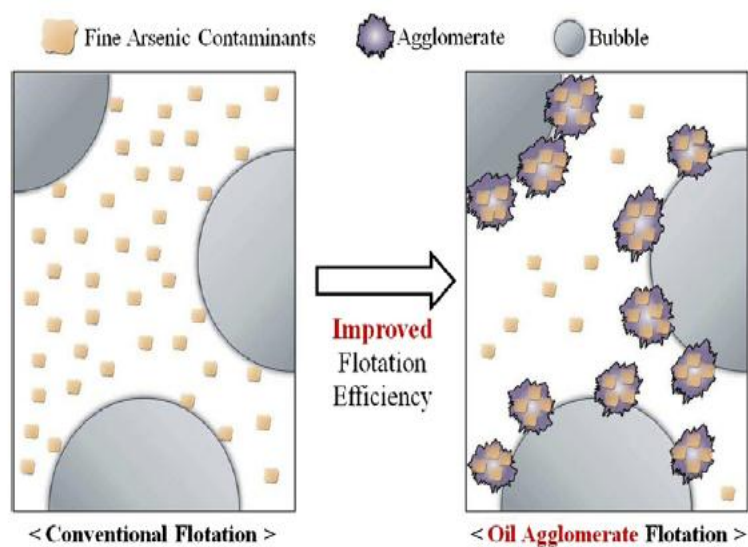
Figure 3 Improved Flotation Effieciency with agglomerate [78]

A study by Morrison and Stasiuk (1998) displayed that the primary bituminous froth contained significant amounts of emulsified water and suspended soil and with an addition of some chemical additives, a higher quality of froth can be produced without jeopardizing froth recovery. Results indicated that a small chemical addition during the nascent froth process led to substantial increase in the capacity of froth handling and treatment [79]. **Figure 4** displays the results obtained in the study.

Table 1 Effects of different additives on froth quality [79]

Additive (4-ml basis)	Primary bitumen recovery %	Primary froth quality		
		Oil %	Water %	Solids %
Blank	80	53	27	20
Toluene	55	57	27	16
Xylene	41	54	26	20
Heptane	52	64	23	12
Toluene/IPA[a]	79	67	19	14
1-Propanol	85	61	23	16
2-Propanol	93	66	19	15
1-Butanol	67	65	20	15
MEK	88	63	24	13
MIBK	58	66	22	12
Formaldehyde	96	65	20	15
Petroleum ether	96	62	22	17
Judy Creek oil	58	66	19	16
Condensate	58	66	19	16

2.2   Microbubbles

The usage of microbubbles has grown with the advancement of technology. Its potential have garnered the interest of a wide range of industries such as bio medical engineering, drug supplement delivery, food processing, water treatment, oil recovery and many others[80].

2.2.1 Microbubbles in industry

The food processing industry is continuously growing massively day by day. There are many activities involving the food processing industry such as mincing, cooking, macerating, emulsification and many more that have benefitted from the application of microbubbles. Protein coated micro bubbles sonochemically generated are used to improve sensory performance for redesigning and formulating ingredients in low fat

foods **[81]**. Other uses for microbubbles in the food industry are residual pesticide flotation, gingerol extraction, and food modification by ultrasound **[82,83]**.

Another industry where micro bubbles have taken by strides is the biomedical field **[84]**. Microbubbles enhance ultrasound energy deposition in tissues and serve as cavitation nuclei thus increasing intercellular drug delivery **[85]**. Accelerated blood clot dissolution in areas of insonation by cooperative action of thrombolytic agents and microbubbles were demonstrated in several clinical trials **[86]**. Other examples of applications for microbubbles in the biomedical industry are as a temporary blood substitutes, providing alleviated blood pressure by reducing exposure to donor donor blood **[87]**, a fluorocarbon emulsion acting as a bridge to transfusion for stroke and myocardial ischemia treatment **[88]** and also to reversibly open the blood brain barrier without damaging the neurons within the cerebal microvasculature for transportation of molecular weight therapeutic compound **[86,88]**.

One of the most prominent fields of application for microbubbles is in the engineering industry where the usage of microbubbles, particularly in waste water treatment and oil removal sector, have been significantly studied in recent times. In waste water treatment plants, microbubbles have help dissolute the oxygen supply to microorganisms in waste water thus improving the rate of water treatment **[89]**. Aside from that, the implementation of microbubble coagulation to enhance the pretreatment effect of dyeing waste water for coloring and oil displayed significantly improvements **[90]**. A schematic diagram of microbubble flotation wastewater pretreatment setup is shown in **Figure 5**.
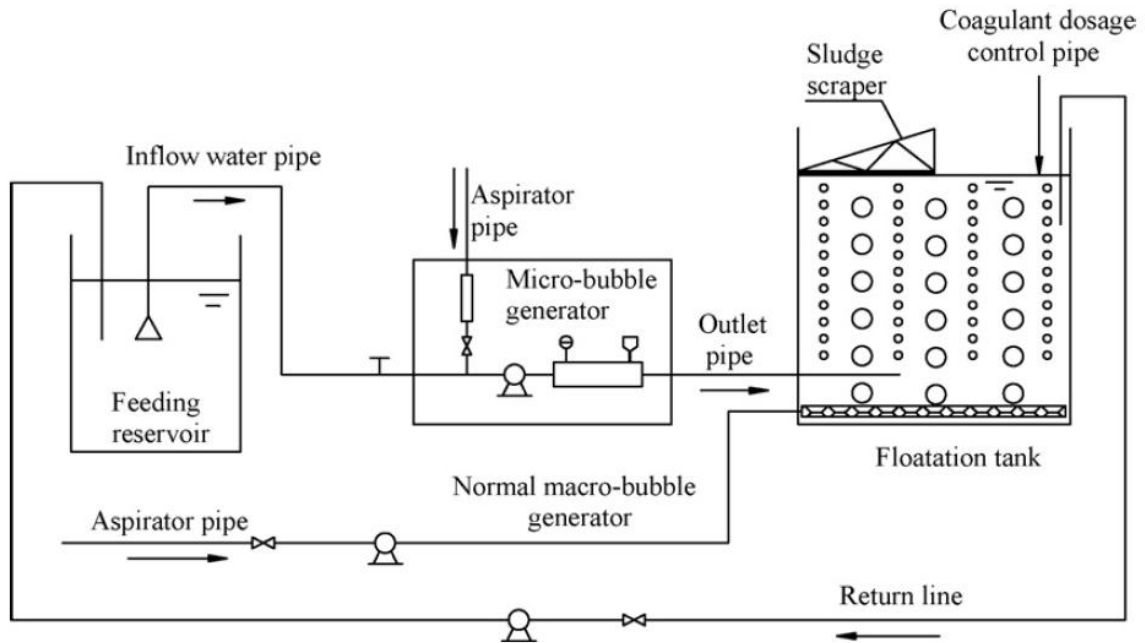
Figure 4 Schematic of microbubble flotation setup for wastewater pretreatment [90]

The oil removal sector is where the applications of microbubble technology have truly shined. Using various methods of generating microbubbles, oil removal and bitumen extraction from contaminated emulsions, soils and other mediums were greatly improved **[91,92]** Hence, the key to successful oil removal is to employ an efficient method of microbubble and a flotation setup that provides maximum contact between bubble and contaminant.

2.2.2 Methods of microbubble generation

In 1985, Ahmed and Jameson performed an investigation to study the effects of bubble size on the flotation recovery on fine particles. From the study result, it is shown that the bubble size greatly affect the recovery rate where a high recovery rate was obtain using small bubble size of $75\,\mu m$ as opposed to large bubble of $655\,\mu m$ [93]. It became apparent that using a suitable method of microbubble generation could greatly improve the oil flotation system.

One method of micro bubble generation is through membrane emulsification. This is done with the use of Shirasu Porous Glass (SPG) membranes which can be prepared by phase separation of the mother glass Na2O–CaO–MgO–Al2O3–B2O3–SiO2, and subsequent acid leaching. It is then subjected to heat treatment within the temperatures ranging from 923K to 1023K for several tens of hours, causing phase separation of the glass to give the acid-insoluble Al2O3–SiO2 and acid soluble Na2O–CaO–MgO–B2O3 phases. The specimen is then submerged into a hydrochloric acid solution resulting in the formation of a porous membrane [94]. The pore size of the membrane can be controlled by adjusting the conditions during the heat treatment phase [95]. **Figure 6** displays a schematic for membrane emulsification microbubble generation.
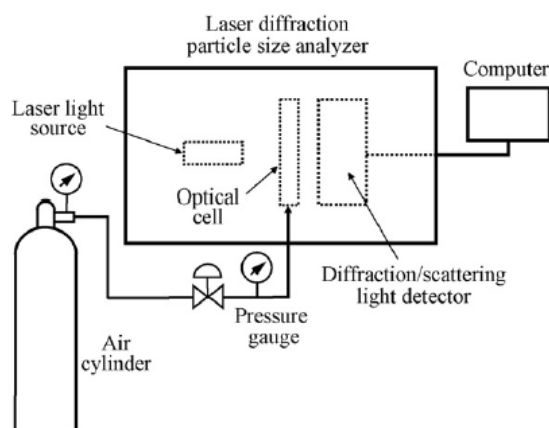
Figure 5 Schematic for membrane emulsification microbubble generation [95]

Another technique of microbubble generation that produces microbubbles with high throughput and improved uniformity is through ink jet printing. The microbubbles are formed by forcing a polymer solution through piezo-driven inkjet nozzles of varying diameters, typically between 20 to 50 μm. Then, by supplying different levels of voltages across the piezoelectric crystal, the pressure generated creates pulses in the solution which leads to the formation of droplets at the nozzle. The inkjet method has advantage over the SPG method due to its ability to vary the bubble size more easily **[96]**. A diagram of microbubble production via inkjet printing is shown in **Figure 7**.
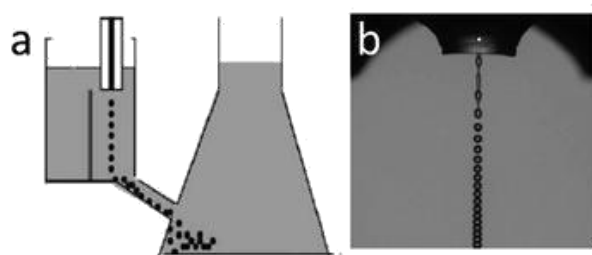
Figure 6 a) Inkjet printing microbubble generation. b) Close-up view [96]

One of the more commonly method of microbubble generation is through sonication. This method involves using high intensity ultrasound to agitate a liquid in a suspension of a suitable coating material **[97]**. The size of microbubbles generated can be varied by adjusting the frequency of the ultrasound. The sonication method of microbubble generation has proven to be the most cost effective and environmentally friendly method **[98,99]**. **Figure 8** displays steps of paclitaxel-coated microbubble production.
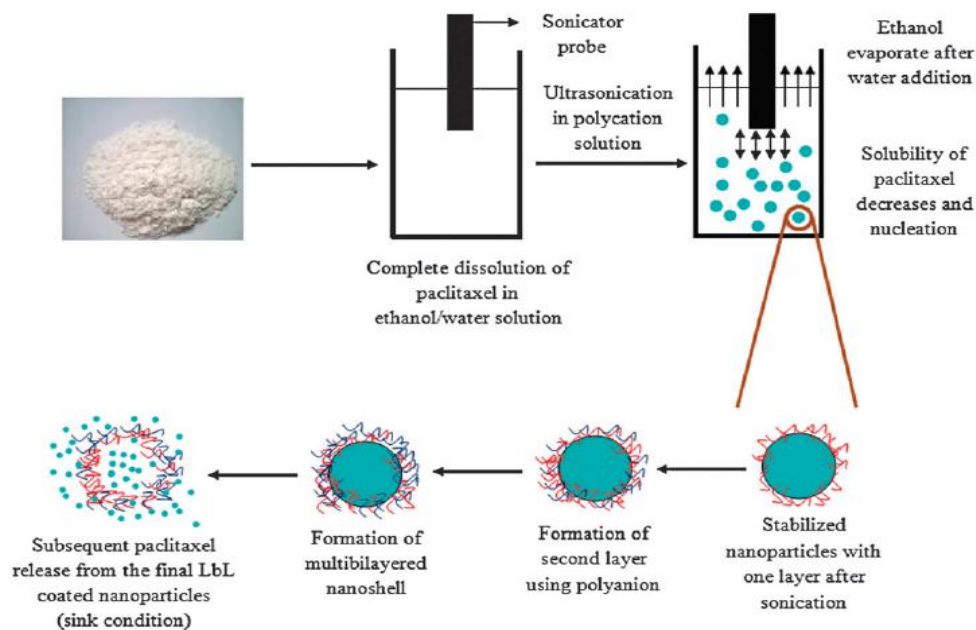
Figure 7 Flow diagram of microbubble generation via sonication for paclitaxel transportation [99]

There are also newly developed methods for microbubble generation such as coaxial electrohydrynamic atomization (CEHDA). This method is an improved approach from the conventional electrohydronamic atomization, where a coaxial jet of two fluids is focused and atomized to form uniform droplets instead of the conventional single stream of liquid, under the influence of an electric field. Provided that the fluids are immisicible, it is then possible to encapsulate one fluid inside the other [100]. For microbubble generation, the two coaxially arranged needles are supplied, one with gas and the other with a liquid of desired coating material, by a pair of precision syringe pumps. An electrical voltage is then applied between the needles and an earthed ring electrode placed a small distance below the tip of the needles [101]. **Figure 9** displays a schematic for CEHDA microbubble generation, as well as a diagram on microbubble generation at the needle. The size of microbubbles is adjusted by varying a range of combinations between the needle flow rates and applied voltage [102].
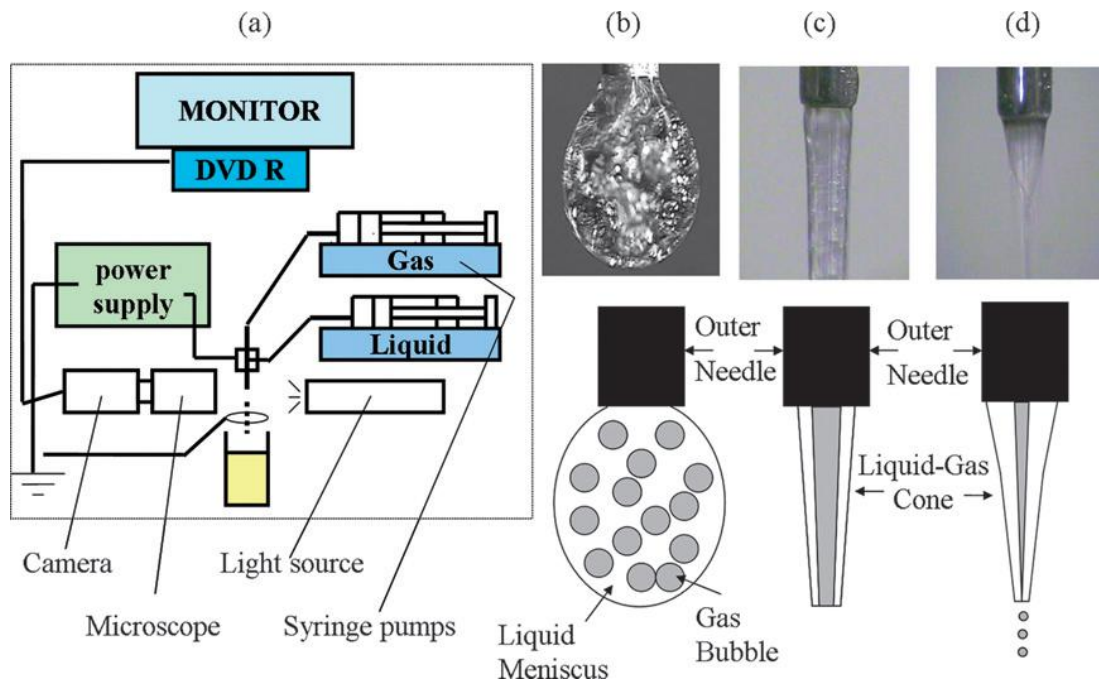
Figure 8 Schematic of CEHDA microbubble generation and flow diagram of microbubble formation [103]

Lastly, another method to generate microbubbles is through micro fluidic devices. Microfluidics is a technology of systems that manipulate small amounts of fluids using channels with dimensions as small as tens to hundreds of micrometers. Microfluidics offers a number of useful capabilities such as the ability to use very small quantities of samples and reagents, and also to produce separations and detections at high resolution and sensitivity. They are also low cost, have short analysis times and small-sized **[104,105]**. The essential feature of a microfluidic device is an orifice where a column of gas impinges over a liquid flow and is focused into a jet. The gas–liquid interface then becomes unstable upon passing the orifice and form bubbles **[106,107]**. The formation of microbubble via a microfluidic device is shown in **Figure 10**, along with a schematic diagram of microbubble generation via a 3-way microfluidic device in **Figure 11**.
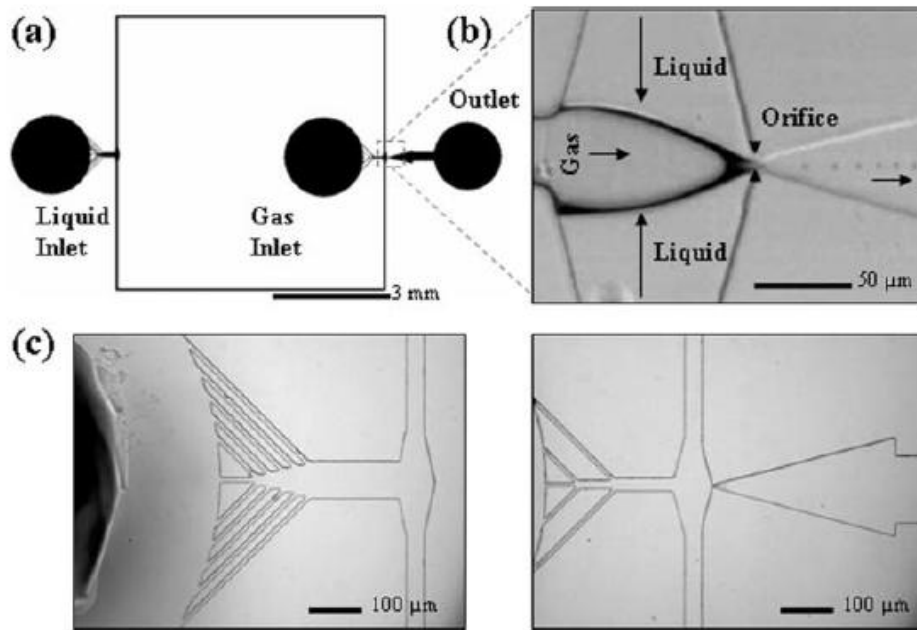
Figure 9 Process of microbubble formation via microfluidic device [108]
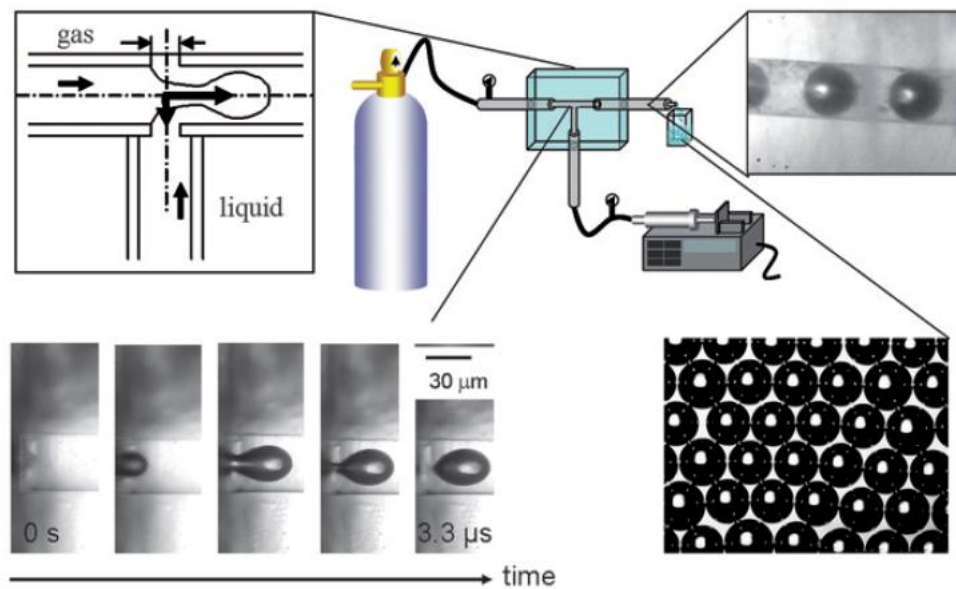
Figure 10 Microbubble generation via 3-way microfluidic device [106]

2.2.3 Coating of microbubbles

Micro bubbles usually consist of 2 components, which is a gas inner core, enclosed by an outer shell **[109].** By coating a microbubble, it provides stability, reduction in

surface tension and surface strength of the bubble hence increasing its lifespan **[110]**. This then allows the bubble to travel and transport the coating substance, a feature that has been widely used in the biomedical field **[109]**. Studies report that coated microbubbles provide longevity and slick movements throughout the human vascular system thus aiding applications such as ultrasound imaging and drug delivery **[111,112]**. The increase strength of the bubbles also aid in therapy studies due to its increase tolerance to acoustic response **[103]**

Therefore, this is a potential application that could significantly benefit the oil removal and remediation of contaminated soil via flotation technology. The increased stability, strength and lifespan will increase the rate of successful particle flotation. Furthermore, the coating substance used could assist in the oil-sand separation phase to further aid the process.

2.3   Graphene

Since the discovery of graphene, it has become the material of much focus for the science and technologies of today. As a two-dimensional atomic structure and a single atom thick arrangement material, graphene exhibits exceptionally high crystal and electronic quality and has already been a source of new physics and potential applications due to its great physical properties and chemical tunability **[113]**. It also possesses great physical properties and chemical tunability thus becoming a great interest for industrial applications.

2.3.1 Graphene in oil adsorption

The large exposed surface area and super-hydrophobic properties of graphene displays excellent potential in terms of oil adsorption **[25]**. Many studies have investigated the oil adsorption capabilities of graphene and applications in the field of oil adsorption. Cote et al (2010) did a study to investigate the possibility to use graphene oxide (GO) as surfactant sheets. Previously considered hydrophilic, it was revealed that GO sheets are actually amphiphilic with an edge-to-center distribution of hydrophilic and hydrophobic domains. Therefore, GO can adhere to interfaces and lower interfacial energy thus acting as a surfactant. In addition, it was also determined

that GO can be used to emulsify organic solvents with water and also disperse insoluble materials such as graphite and nanotubes (CNT) in water [114].

The unique microstructure of graphene also be shaped into a sponge-like structure capable of absorbing oils and organic solvents. Its unique structure and toughness provide high efficiency and recyclability [115]. An investigation by Bi et al (2012) displayed that a graphene sponge could absorb not only petroleum products and fats, but also toxic solvents such as toluene and chloroform, without the requirement of any further treatment. Furthermore, the graphene sponge could be regenerated by simple heat treatment. Graphene could also be shaped into foam for better dispersion hence better contact with contaminants [116,117]. This can be attributed to strong electrostatic repulsion between graphene particles allowing for uniform and homogenous dispersions. The viscosity and surface of graphene-water fluid could also be manipulated as they react inversely proportional to temperature [118].

He et al (2013) also investigated the fabrication of graphene oxide foams in search for an environmentally friendly method to produce reduced graphene oxide (RGO) foam with a high oil absorption capacity. Three different fabrication methods were employed; unidirectional freezing drying (UDF), non-directional freezing drying, and air freezing drying. The absorption rate of both GO foams and its reduced forms were tested and it was determined that RGO foams were hydrophobic and displayed significantly higher absorbing capabilities. The absorption capacity of the RGO foams made by UDF was higher than $100 \, \mathrm{g \, g^{-1}}$ for all the oils tested (gasoline, diesel oil, pump oil, lubricating oil and olive oil) and registered the highest value of about 122 $\mathrm{g \, g^{-1}}$ for olive oil. The oil absorption capacity of the GO foams was found to be lower than that of the RGO foams [117]. Results obtained can be seen in **Figure 12**.
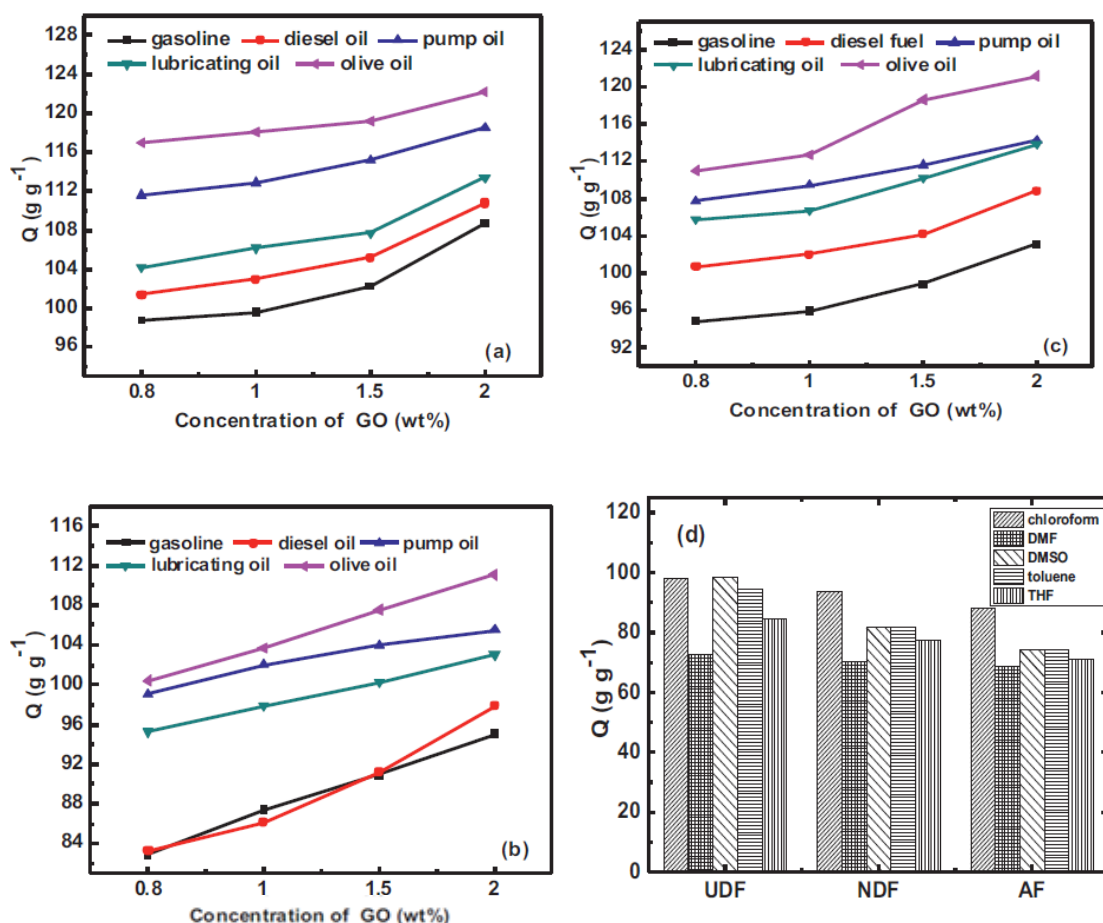
Figure 11 Oil adsorption capacity of GO against gasoline, diesel oil, pump oil, lubricating oil and olive oil [117]

Graphene can also be magnetized in order to be easily handled with a magnet. This would allow graphene foam or dispersed graphene to adsorb oil and solvent particles and then be collected using a magnet [**119**]. Yang et al (2014) conducted an experiment with this method using graphene oxide foam loaded with magnetite nanoparticles (Fe_3O_4).The graphene foam manifested outstanding oil adsorption capacity, high restoration for absorbates and excellent recyclability and stability under cyclic conditions. **Figure 13** displays oil absorption using magnetic graphene and then graphene foam removal using a magnet.
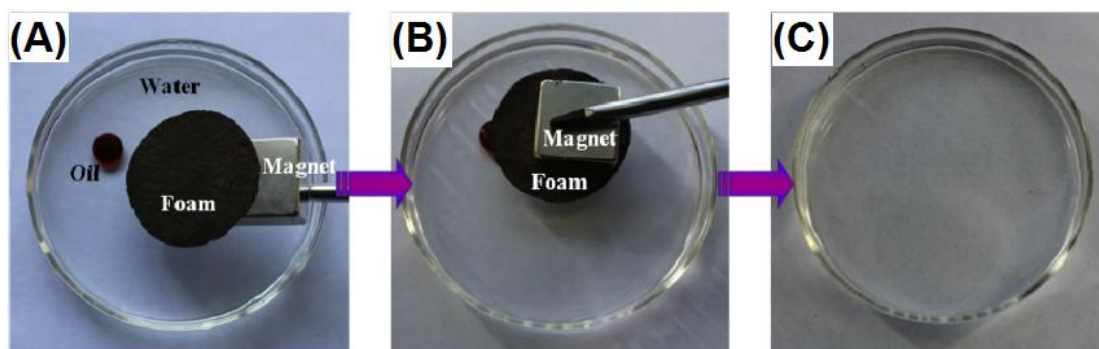
Figure 12 Oil absorption using magnetic graphene [119]

Graphene could also be manipulated in aerogel form or nanosheet form depending on the required shape thus making it easy to use. Graphene in aerogel form exhibit outstanding adsorption efficiency with low density and thermal conductivity [120]. In nanosheet form, graphene was able reduce surface tension between oil and water. The graphene was also able to form a layer in between the oil phase and water phase thus separating them from one another [121,122]

Many studies improve on graphene oil adsorption by manipulating the structure of graphene particles, but also other factors involved, such as pH levels and oil-sand separation rate. Studies have shown that zeta potential measurements can be used to measure the attractive forces between solid particles immersed in a liquid [123] and the ability to manipulate these values through the variation of pH levels [124]. These studies were then used to investigate interactions between contaminants and bubbles used in flotation technology [125,126]. In 1995, Dai and Chung showed that under alkaline conditions, bitumen-sand separation rate was higher as this counteracts the natural acidity of oil [127]. With this, the efficiency of graphene in oil flotation could be further improved [126,128].

Besides pH level manipulation, other research has gone into investigating the effects of interfacial tension, density, viscosity and temperature with respect to graphene. The introduction of graphene to the oil-bubble interface would reduce interfacial tension thus improving the separation of oil particles [118,129]. An increase of temperature would also benefit graphene supplemented flotation as the density and viscosity decreases [130,131]. A study by Schramm et al (2002) displayed the effects of interfacial tension on the recovery of bitumen by water-based conditioning and flotation, and displayed that optimal recovery was found when the bitumen/aqueous

23

interface had maximum interfacial electric charge and minium interfacial tension **[66]**. Therefore, there is still much potential in graphene to further improve the oil flotation process.

CHAPTER 3: MATERIALS AND METHODOLOGY

3.1   Materials

The Graphene Nanoparticle Powder (GNP) used in this experiment is Nanostructured Graphite-250 purchased from Graphene Supermarket online store. The properties of the graphene purchased are listed in the Table 2.

Table 2 GNP specifications

Specific surface area	$250 \text{ m}^2/\text{g}$
Lateral size	100-500 nm
Thickness	10-300 nm

MFO 180 crude oil (viscosity of 180 cst) was obtained from KIC Terminal, Port Klang. This oil was mixed with sand samples to the prepared contaminated sand used in this experiment.

The sand samples used in this experiment was obtained from the shores of Port Klang, Malaysia. The sands procured will be mixed with crude oil to prepare the contaminated sand samples used in this experiment.

Sodium hydroxide pellets (NaOH, Sigma Aldrich, $\geq$ 98%) were obtained from Monash University Laboratory. These were used to obtain different pH levels required for this experiment.

3.2   Methodology

3.2.1 Preliminary tests – Zeta Potential Measurements

The aim of this phase is to determine the effects of pH levels on the graphene nanoparticles and microbubbles attachment. In the graphene supplemented oil recovery flotation method, the hydrophobic graphene nanoparticles is suggested align themselves around the hydrophobic microbubbles, thus enhancing the oil attachment to the graphene adsorbing microbubbles and subsequently flotation of oil to the surface. At the same time, the GNP dispersion is also suggested to accelerate the dislodging and separating of oil from sand particles through reduction of interfacial tension between the oil and GNP dispersion.

3.2.1.1 GNP dispersions preparation

0.5 g of GNP was mixed with 0.5 litre of distilled water to obtain a 0.01 wt% concentration. The GNP samples were then sonicated for 20 minutes to disperse the graphene nanoparticles inside the distilled water in order to obtain homogenous pure graphene dispersion. The samples were then allowed to sit and cool down for an hour in order to bring the sample to room temperature and eliminate any presence of microbubbles in the graphene solution.

3.2.1.2 Microbubble solution preparation

Distilled water was sonicated for 20 minutes, and instantaneously brought into the zeta sizer for zeta potential measurements without cooling.

3.2.1.3 Heavy crude oil droplets preparation

0.5 g of oil was mixed with 0.5 litre of distilled water to obtain a 0.1 wt% concentration. The oil droplet sample was then sonicated for 20 minutes to disperse the graphene nanoparticles inside the distilled water in order to obtain homogenous pure oil dispersion. The samples were then allowed to sit and cool down for an hour in order to bring the sample to room temperature and eliminate any presence of microbubbles in the graphene solution.

3.2.1.3 Titration level control

Sodium hydroxide pellets were mixed with distilled water and shaken vigorously to dilute the NaOH. Once this is done, the graphene and microbubble solution samples with pH levels 6 to 11 were prepared. This is done by using a dropper to introduce NaOH and monitoring the titration levels through a pH probe meter. Titration level control setup is shown in **Figure 14**.

Figure 13 Titration level control setup

3.2.1.4 Zeta potential measurements process

Zeta potential is known as the potential difference that exists between the surface of a solid particle immersed in a conducting liquid and the bulk of the liquid. The zeta potential of the graphene and microbubble solutions at varying pH levels were measured using the Zeta Sizer Nano S90 (Model: Malvern Instruments Ltd., UK).

Once the graphene and oil droplet solution has cooled for 30 minutes to eliminate the presence of microbubbles in the solution, a sample was injected in the zeta sizer cell, displayed in **Figure 15,** which would then be placed in the reader,displayed in **Figure 16,** in order to obtain a zeta potential measurement. This was repeated 3 times for each sample. Aside from the cool down period, the process was repeated for in order to obtain the zeta potential measurements for the microbubble solutions.

Figure 14 Zeta sizer sample cell

Figure 15 Zeta sizer

3.2.1.5 Analysis of Zeta potential measurements

Zeta potential measurements are a key indicator of the stability of colloidal dispersions. It is used to indicate the degree of electrostatic repulsion between adjacent, similarly charged particles in dispersion. Therefore, it is key to determine the rate of attachment of graphene to microbubbles against pH levels. Once all the zeta potential measurements from both the graphene solutions and microbubble solutions were completed, the results would be analyzed to verify the interaction between graphene nanoparticles and microbubbles once they come into contact. Particles can only be positively charged or negatively charged therefore only 3 types of outcome would be possible and they are:-

1. Both graphene and microbubble solutions are positively charged.
2. Both graphene and microbubble solutions are negatively charged.

3. Graphene and microbubble solutions are oppositely charged.

When they have opposite charges, this would signify attraction between one another and would help graphene particles attach to microbubbles and assist in the oil recovery process. The level of repulsion between microbubble and graphene can be observed by the magnitude difference of zeta potential between the charges.

When both graphene solution and microbubble solution have the same type of charge, they will repel from one another and therefore not a wanted quality to enhance the oil recovery efficiency. However, for molecules and particles that are small enough, with a low zeta potential, Van Der Waals attractive forces may exceed this repulsion and the dispersion can break and clump together in a floc, known as flocculation **[123,124]**. The behaviour of the colloid at different levels of zeta potential is displayed in the **Table 2**.

Table 3 Stability behaviour of colloid at different zetapotential levels [124]

Zeta Potential, mV	Stability behaviour of colloid
from 0 to ±5,	Rapid coagulation or flocculation
from ±10 to ±30	Incipient instability
from ±30 to ±40	Moderate stability
from ±40 to ±60	Good stability
more than ±61	Excellent stability

3.2.1.6 DLVO Theory

The Derjaguin-Landau-Verwey-Overbeek theory (DLVO theory) is named after Boris Derjaguin, Lev Landau, Evert Verwey and Theodor Overbeek and explains the aggregation of aqueous dispersions quantitatively and describes the forces between charged surfaces interacting through a liquid. This is done by combining the effects of the van der Waals attraction as well as electrostatic repulsion.

The DLVO theory would be used to confirm the behaviour of GNP and microbubble solution at different pH levels. The DVLO theory used to measure inter particle forces was calculated assuming a silica water bitumen system. This theory states that the sum of total energy of a system, FT equals to sum of electrical double layer repulsive force, and sum of Van Der Waals force of attraction, F_A [127].

$$F_T = F_R + F_A \tag{1}$$

$$F_R = -\frac{dV_R}{dH} = \frac{\varepsilon a \kappa e^{-\kappa H}}{2(1-e^{-\kappa H})}\left[2\zeta_1\zeta_2 - e^{-\kappa H}\left(\zeta_1^2 + \zeta_2^2\right)\right] \tag{2}$$

$$F_A = -\frac{dV_A}{dH} = \frac{aA\,\lambda(\lambda+28H)}{6H^2(\lambda+14H)^2} \tag{3}$$

$$\kappa = \left(\sqrt{\left(\frac{e^2}{\varepsilon kT}\right)}\right)\Sigma_i z_i^2 c_i N_i \tag{4}$$

Where,

ε = Permittivity of a medium

a = Radius of the micro bubbles (1×10^{-6}m)

A = Combined Hamaker constant for graphene/water/microbubble (1.565×10^{-20}J)

ζ_1 = Measured zeta potential for micro bubbles (mV)

ζ_2 = Measured zeta potential for graphene (mV)

λ = Characteristic wavelength of interaction (100nm)

H = Separation distance

κ = Deybe constant

e = Elementary charge ($1.602 \times 10^{-19}C$)

k = Boltzman constant (1.381×10^{-23})

NA = Avogadro number (6.022×10^{23})

T = temperature in Kelvin

z_i and c_i is molar concentration in mol/m^3

The combined Hamaker constant for two different particles interacting in a third medium was obtained following Hamaker's pair-wise summation procedure. The Hamaker constants for graphene, microbubbles and water in vacuum were determined and combined using the following formula [132]:-

$$A_{132} = A_{12} + A_{33} - A_{13} - A_{23} = \left(\sqrt{A_{11}} - \sqrt{A_{33}}\right)\left(\sqrt{A_{22}} - \sqrt{A_{33}}\right) \qquad (5)$$

Where,

A_{11} = Hamaker constant of graphene, 29.65×10^{-20} J   **[133]**

A_{22} = Hamaker constant of microbubbles, 5.61×10^{-20} J   **[134]**

A_{33} = Hamaker constant of water, 3.7×10^{-20} J   **[133]**

3.2.2 Characterization of GNP dispersions

The characterization studies were conducted with GNP concentration of 0.001 wt%, 0.005 wt%, 0.01 wt%, 0.025 wt%, 0.05 wt% and 0.1 wt% mixed with 1litre of distilled water. To homogeneously disperse the GNP into the distilled water, the GNP/water mixture was sonicated for 5 minutes. Density, interfacial tension, viscosity and pH measurements were taken. Every test was replicated at least three times.

3.2.2.1 Density and interfacial tension measurements

The density of GNP dispersions and 180 cst crude oil was measured using the force tensiometer (Model: Attension Sigma 702), shown in **Figure 17**, using a density probe. The density of GNP concentration at 0.001 wt%, 0.005 wt%, 0.01 wt%, 0.025 wt%, 0.05 wt% and 0.1 wt% was obtained. Similarly, the density for 180 cst crude oil at different temperature levels was measured. A hot water bath was used to maintain the temperature levels at 25 ℃, 40 ℃, 60 ℃ and 80 ℃.

The interfacial tension between the 180 cst crude oil and GNP/water mix was also measured. Using the Du Noüy ring method, this is done by measuring the force required to slowly lift a ring, usually made of platinum, from the surface of the liquid to measure the surface tension of a liquid. To measure the interfacial tension between

180 cst crude oil and GNP/water mix, the starting position of the ring is placed at the interface between both liquids. The interfacial tension between the 180 cst crude oil and GNP water was measured at different temperatures of 25.6 ℃, 40 ℃ and 60 ℃ and 80 ℃ at 0.1 wt% GNP water only, using a temperature bath.

Figure 16 Force Tensiometer (Model: Attension Sigma 702)

3.2.2.2 Viscosity measurements

The viscosity of the GNP/water mix was also measured using a rheometer (Model: AMETEK Brookfields), shown in **Figure 18**. The viscosity at different temperature of 25.6 ℃, 40 ℃ and 60 ℃ and 80 ℃ at 0.1 wt% GNP/water mix was measured.
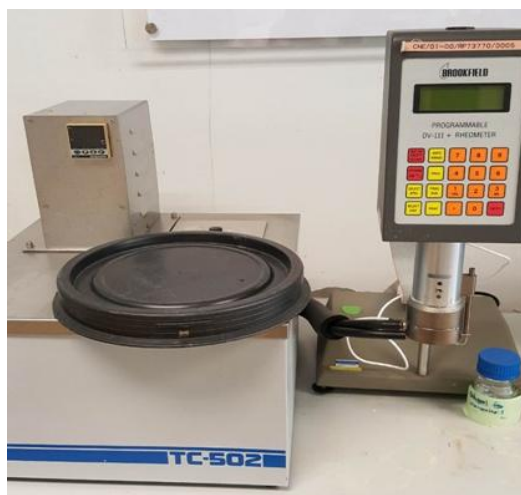
Figure 17 Rheometer (Model: AMETEK Brookfields)

3.2.2.3 pH measurements

The Effects of the GNP on pH levels was also measured in this study. A pH meter (Model: Mettler Toledo Five Easy Plus),shown in **Figure 19**, was used to measure the pH values at different GNP concentration levels and also at different temperature levels. The pH levels of GNP concentration at 0.001 wt%, 0.005 wt%, 0.01 wt%, 0.025wt%, 0.05 wt% and 0.1 wt% and at temperature levels of 25 ℃, 40 ℃, 60 ℃ and 80 ℃ were measured.

Figure 18 pH meter (Model: Mettler Toledo Five Easy Plus)

3.2.3 GNP supplemented microbubbles oil flotation efficiency studies

The efficiency of GNP supplemented microbubbles oil flotation against pH levels, GNP concentration, and temperature were investigated. A laboratory scale oil

flotation setup, using a venture tube for microbubble generation was built to investigate the effects of GNP concentration, pH and temperature on oil removal efficiency.

3.2.3.1 Contaminated sand sample preparation

2kg of raw sand was first washed in a 5 litre beaker using 2 litre of distilled water to remove dust particles and debris from the sample. This process was repeated 3 times to ensure that all dust particles and debris were removed from the sand sample. The wet-sands are then transfer beakers and dried in the oven for 2 hours at 130 ℃ to remove any moisture from the sand and then allowed to cool down back to room temperature. The sand was sieved using the Retsch AS 200 sieve shaker in order to separate them into different sizes. Sieves of 1mm, 500 μm, 250 μm and 125 μm opening mesh size were used to distribute the sand into different particle sizes.

The contaminated sand samples for this experiment were prepared by mixing the sand with the crude oil according to the ratio of 5:2; 125 g of sand is mix with 50 g of 180 cst crude oil in a 500 ml beaker. Sand samples are prepared using 1mm, 500 μm, 250 μm and 125 μm sand sizes at ratio of 6:2:1:1 to mimic actual soil as summarised in **Table 3**. The Retsch AS 200 sieve shaker, which employs the American Society for Testing and Materials standards (ASTM), was used in this experiment.

Table 4 Sand diameter composition for contaminated soil

1 mm	1 mm – 2 mm	6	75
500 μm	500 μm – 1 mm	2	25
250 μm	250 μm – 500 μm	1	12.5
125 μm	125 μm – 250 μm	1	12.5
			$\Sigma = 125$

3.2.3.2 Laboratory scale microbubbles oil flotation setup

The microbubble flotation rig used in this study is a laboratory scale flotation column. It consists of a reservoir tank, a flotation column, a venturi tube, a centrifugal pump, a peristaltic pump, a ball valve and a rotameter as seen in the schematic show in **Figure 20**. The reservoir tank serves as storage and supplies water which is pump throughout the system by the centrifugal pump. Water is pumped in a close loop where the

peristaltic pump will return water back to the water storage tank. This flotation column design was adopted from a study conducted by Lim et al (2015). The microbubbles are generated by inducing air into the throat of the venture tube through a syringe needle using hydrodynamics cavitation venture tube method while water is pumped through the venture tube. The level of water in the water tank can be controlled by adjusting the inlet flow rate, controlled by the ball valve, and the outlet flow rate, adjustable via the peristaltic pump.
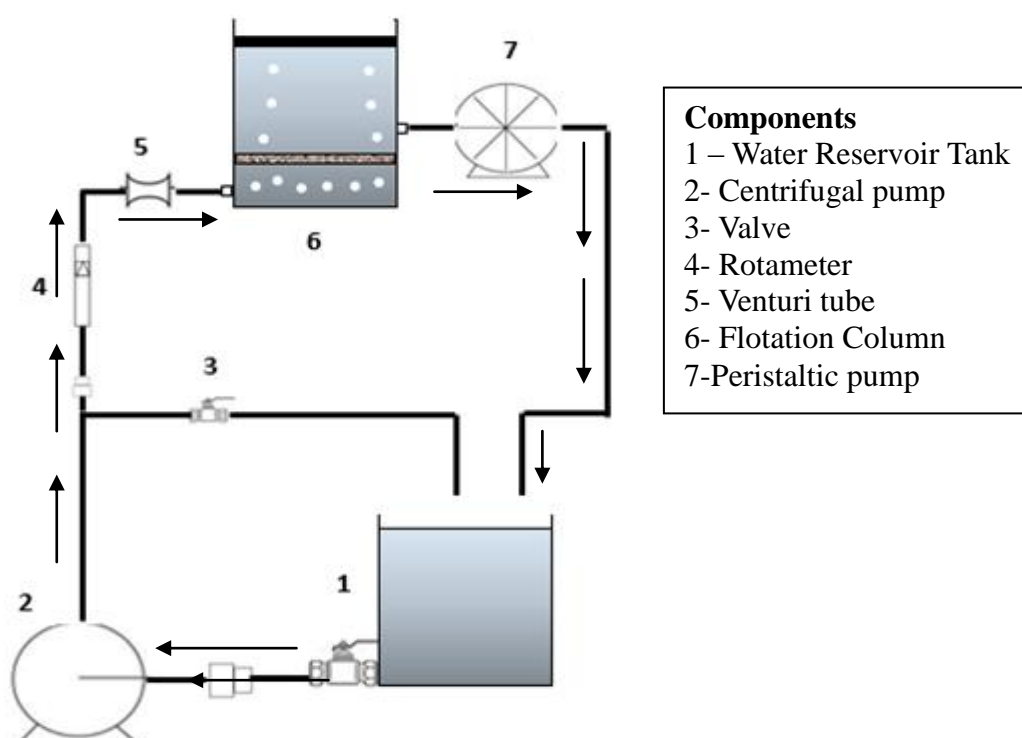
Figure 19 Schematic of laboratory scale flotation setup

3.2.3.2 Effects of GNP concentration

To investigate the effects of GNP concentration, a total of six different levels of weight concentration were used. These levels were measured in weight percent (wt %) where the weight of GNP applied was calculated based on the percentage of contaminated sand weight. Levels of GNP concentrations used were 0.01 wt%, 0.05 wt%, 0.1 wt%, 0.25 wt%, 0.5 wt% and 1 wt%. The mass of the GNP are weighted using the analytical balance (Model: METTLER TOLEDO) balance that has an accuracy of ±0.0001 g.

The GNP was then dispersed into 8 litre of distilled water and transferred to the reservoir tank. The mixture of GNP and water would then be circulated throughout the system via pumps. The contaminated sand sample was placed on a fine mesh sieve and then on to a platform elevated 10 cm tall was placed at the bottom of the flotation column. The hose exiting the centrifugal pump was connected to the venturi tube which was connected to the bottom inlet of the flotation column. This will allow the GNP/water mix to be pumped through to the bottom of the flotation column. 2 litres of distilled water is then from above the flotation column to submerge the contaminated sand sample. This will add up to a total of 10 litres of distilled water in the system. Another hose is attached to the middle exit of the flotation column to the peristaltic pump in order to cycle the GNP/water mix back to the reservoir tank.

For this test, the centrifugal pump is switched on and the flotation process was allowed to run for 30 minutes. The oil that floats up when the GBP/water mix is cycled through the contaminated sand sample was collected. The test was conducted 3 times to achieve the best possible results.

3.2.3.3 Effects of pH levels on oil removal efficiency

The aim of this phase is to determine the effects of pH levels on graphene supplemented microbubble flotation method for oil removal. As oil particles are naturally acidic and negatively charged, they tend to attract sand particles which are positively charge albeit in small amounts. Therefore, under alkaline conditions, the oil particles will become positively charged and begin to repel sand particles hence improving oil-sand separation and recovery [125,126,127].

Samples with the optimum GNP concentrations obtained from the previous phase were used in this experiment. Using the similar setup and procedure, the samples were prepared and tested against pH levels from 6 to 11. 5 samples were prepared and the experiment was repeated 5 times for each pH level. A pH probe meter was used to monitor the pH levels throughout each experimental run.

3.2.3.4 Effects of temperature

Based on the GNP concentration and pH level experiment, the optimum amount of graphene determined was used for this test at the optimum pH level. Using the similar

setup, the oil removal efficiency at water temperatures of 40 ℃, 60 ℃ and 80 ℃ was tested to determine an optimum temperature for oil recovery. In this investigation, the water was heated up until the desired temperatures before being poured into the tank reservoir. A mercury thermometer was used to monitor the water temperature in the reservoir. The experiment was repeated 3 times.

3.2.3.5 Oil recovery efficiency

Once an experimental run is completed, oil floated to the surface of the container is skimmed and pumped out, along with a portion of water remaining, into a beaker and disposed. The remains of the sample are then heated in an oven overnight to remove any remains of water. This leaves only sand and unfloated oil remaining. This weight is then measured and compared with the original weight of the sample of oil/sand to dertermine the amount of oil removed by flotation. Therefore, the oil recovery efficiency was calculated using equation (5):-

$$\textbf{Oil recovery efficiency } (\%) = \frac{\textbf{Weight of recovered crude oil(g)}}{\textbf{Total weight of crude oil (g)}} \times \textbf{100}\% \tag{5}$$

CHAPTER 4:   RESULTS & DISCUSSIONS

4.1   Zeta potential measurements

4.1.1 Zeta potential measurement of GNP dispersions
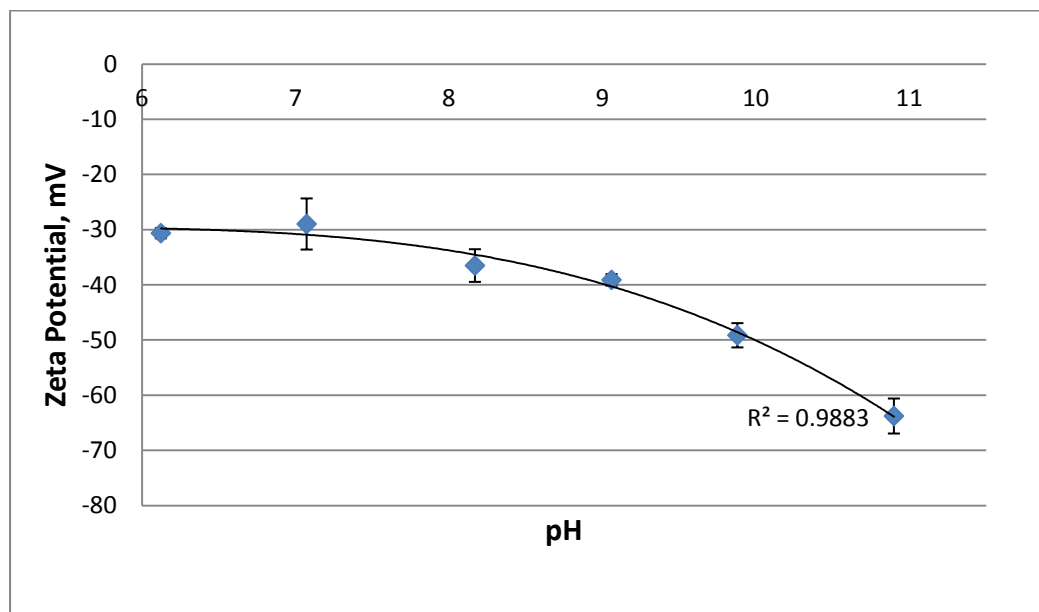
Figure 20 Zeta potential measurement of GNP dispersion

Based on **Figure 21**, it can be seen that the zeta potential of GNP solution decreases exponentially as the pH level increases. Similar studies also indicated that the zeta potential of graphene dispersion was negative under neutral conditions and only increase in magnitude due to the increase in pH **[118]**. GNP solution between pH levels 6 to 9 are at moderate stability zeta potential levels, 30.6 mV at pH6 and 39.1 mV at pH 9. However, from pH levels 9 onwards, the zeta potential magnitude increases and thus becomes more stable and increasing in repulsion of other particles **[123,124]**. This makes it more difficult for graphene particles to attach to microbubbles which would result in lower oil recovery efficiency.

4.1.2 Zeta potential measurement of microbubble solution
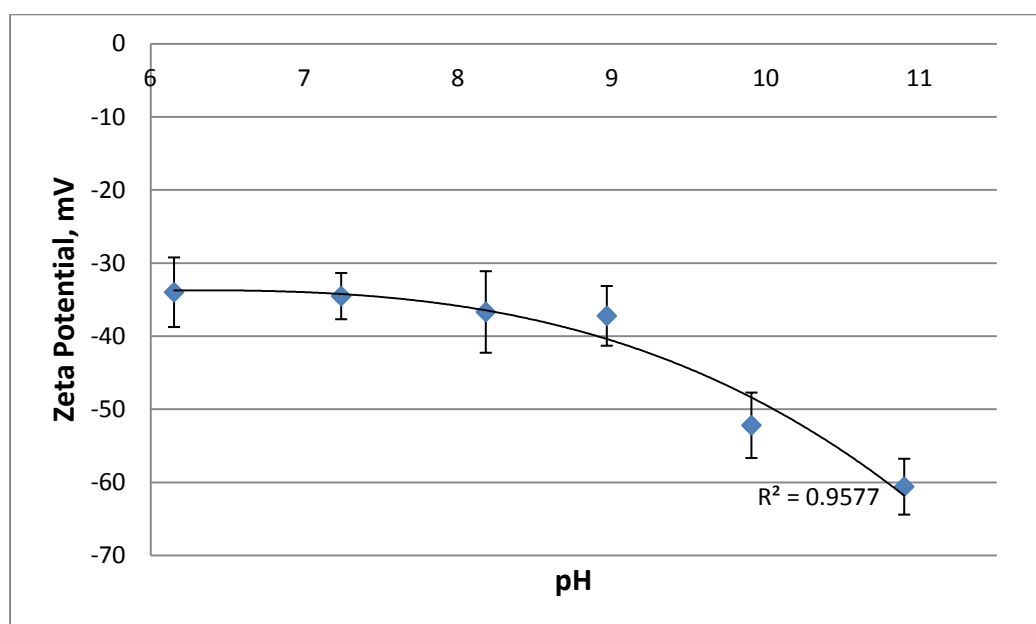
Figure 21 Zeta potential measurement of microbubble solution

In **Figure 22**, microbubbles solution via sonication displays similar characteristics. The zeta potential decreases, increasing in magnitude exponentially, as pH level increases. This trend was found to be similar with findings in **[125].** The zeta potential of microbubble solution remains in the moderate stability region of ±30 to 40 mV from pH levels 6 to 9. The zeta pontential at pH6 was at -34 mV and slowly decreases to -37.2mV at pH 9 before increasing drastically into the exceptional stability range, 60.6 mV at pH 11.

Therefore, based on **Figures 21 and 22**, as pH levels increase, the zeta potential magnitude of both graphene and microbubbles increase, hence the repulsion between them will also increase. This will cause the rate of attachment between microbubble and graphene to drop thus reducing their effectiveness in assisting oil flotation.

4.1.3 Zeta potential measurement of heavy crude oil droplets
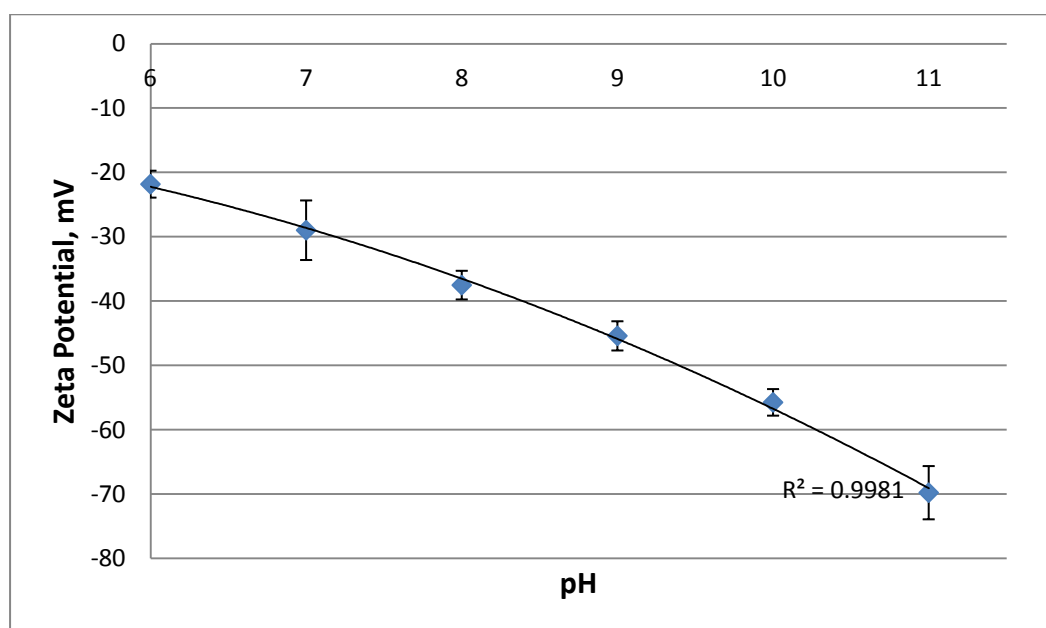
Figure 22 Zeta potential measurement of heavy crude oil droplets

Similar to the zeta potential measurements of GNP dispersions and microbubble solution, the zeta potential of heavy crude oil droplets in **Figure 23** displays a negative zeta potential value decreasing exponentially with pH levels. The lowest registered zeta potential value measured for heavy crude oil was -21.8 mV at pH 6. The zeta potential value decreases exponentially and measures at -69.77 mV at pH11.

Unlike the zeta potential of GNP dispersions and microbubbles, the zeta potential of heavy crude oil droplets is within the incipient instability range (-10 to -30 mV) between pH 6 and 7. This indicates that the pH level for graphene and microbubbles to attach with oil particles is at pH 6 to7. Hence, the optimum pH level for graphene supplemented microbubble oil flotation would be at a neutral pH.

In essence, this indicated that oil particles would inherently attach to the microbubbles at pH 6 to 7 due to hydrophobicity, with or without the addition of graphene nanoparticles. Therefore, further experimentations were conducted to verify the effects of GNP supplementation in the oil flotation process.

4.1.4 DLVO Theory

DLVO theory was used to quantitatively display the effects of pH levels on the graphene-microbubble attachment. Based on the measured zeta potentials of GNP dispersions and microbubble solutions, it was concluded that graphene-microbubble attachment difficulty increases with pH. Using DLVO theory, the van der Waals attraction and the electrostatic repulsion between charged graphene and microbubbles surfaces were calculated to determine the total inter particle force that occur **[135]**. This force will determine the degree of attachment between graphene particles and microbubbles.
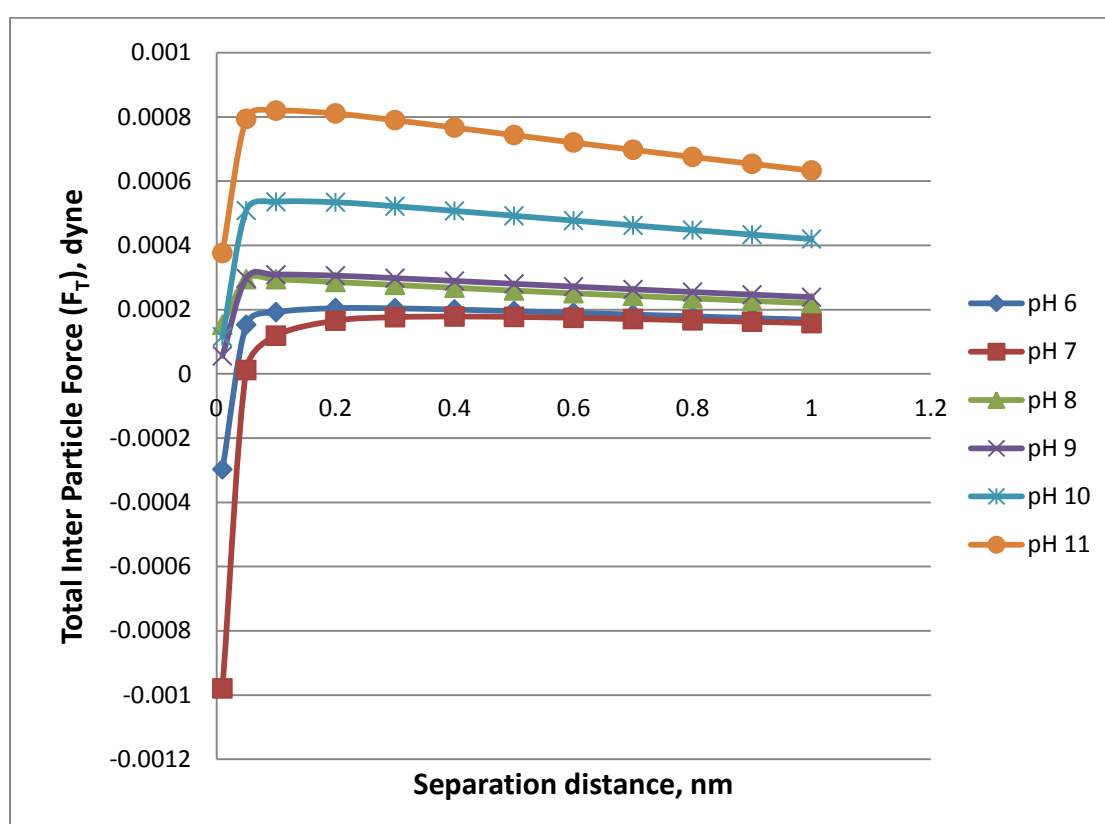
Figure 23 Total inter particle force against separation distance at different pH levels

Using DLVO theory, the total inter particle force (F_T) was tabulated against particle separation distance (H) at respective pH levels as seen in **Figure 24**. Positive F_T values indicate repulsive forces while negative values display an attraction force. Also, it can be seen that pH 6 and pH7 were the optimum pH levels as they had attractive forces at low separation distances. Furthermore, at larger separation distance, the

repulsive forces were minimal at pH 6 and 7. This suggests that pH 6 to pH 7 is the preferential region for optimum graphene-microbubble attachment.
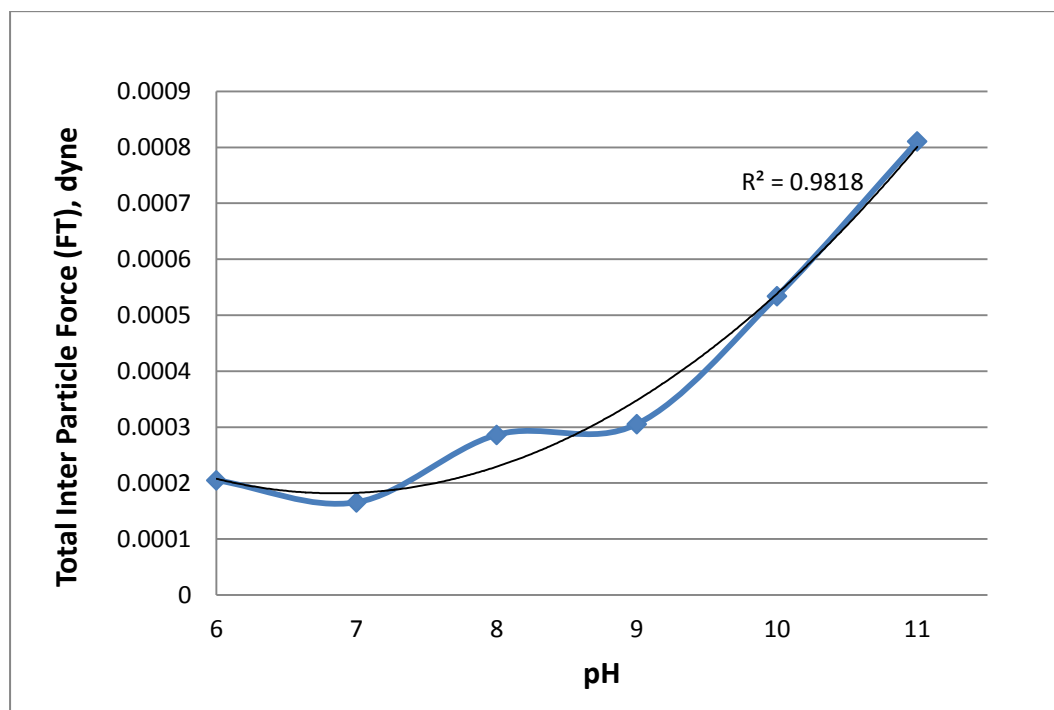
Figure 24 Total inter particle force against pH at separation distance of 0.05 nm

According to **Figure 24,** F_T values peak around the separation distance (H) of 0.05 nm and then begins decreasing as the separation distance increases. **Figure 25** shows the F_T between graphene and microbubbles at separation distance of 0.005 nm. From pH 6 to 7, F_T values remain around 0.0002 dyne. The F_T increases drastically once it passes pH 9 indicating strong repulsive forces not ideal for graphene-microbubble attachment. Therefore, this result correlates with findings in **4.1.2** and **4.1.3,** that graphene-microbubble attachment becomes more difficult as pH levels increase, and attachment to oil droplets is strongest at neutral pH levels.

4.2   Characterization studies

4.2.1 Density measurements
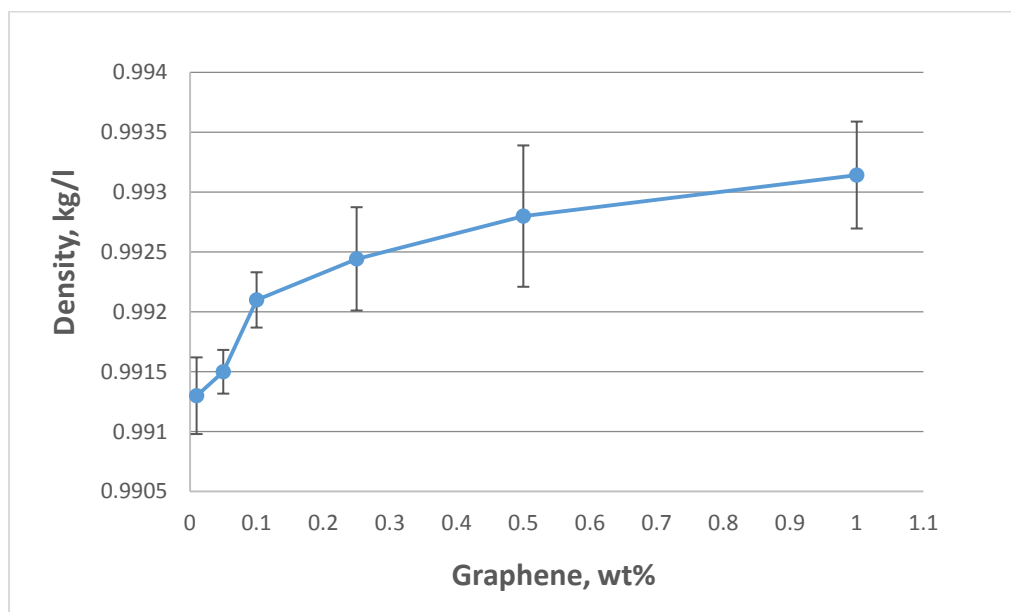
Figure 25 GNP dispersion density against graphene concentration

Figure 26 shows the density of GNP dispersions at room temperature in water (pH 7) at different levels of GNP concentration. It can be seen that concentration of graphene in water increases, the density of the mixture increases. As density is a function of mass per volume, this is proven to be true.

4.2.2 Interfacial tension measurements

In order to further understand the interactions between the crude oil and GNP dispersions, the interfacial tension (IFT) between both liquids were investigated. The interfacial tension between GNP dispersions and crude oil against GNP concentration levels and temperature levels were investigated and the results obtained were tabulated and plotted.
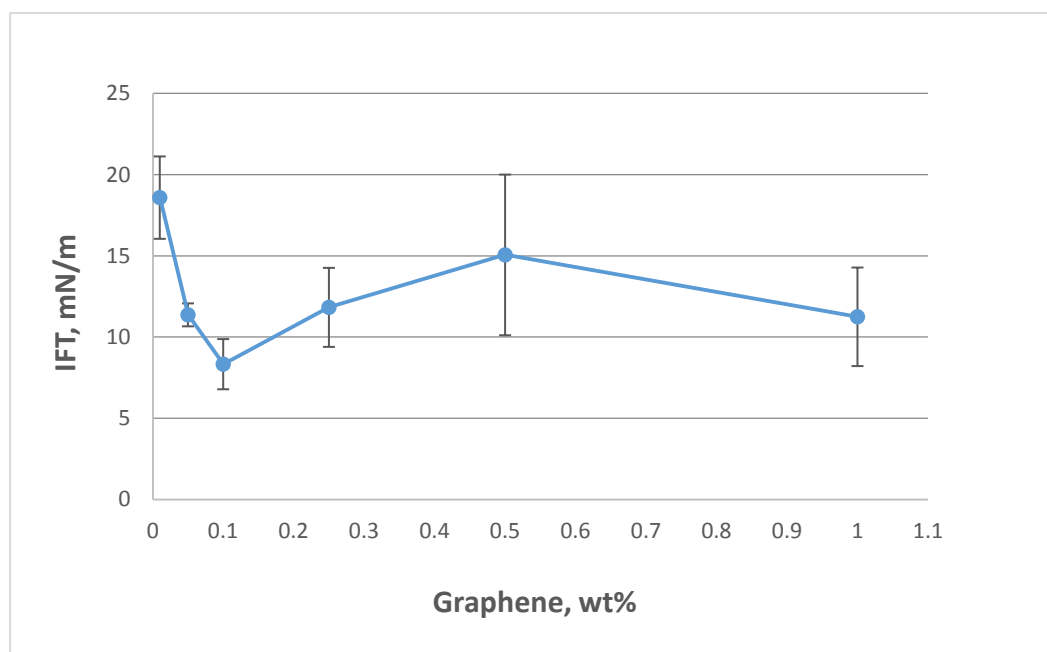
Figure 26 Interfacial tension against GNP concentration

Results demonstrated in **Figure 27** indicated that the interfacial tension reduces to a minimum of 8.385 mN/m when the GNP concentration to 0.1 wt%. This shows that at 0.1 wt% of GNP, the presence of graphene would accumulate at the crude oil/water interface, causing a reduction of the interfacial area which resulted in a lower interfacial tension [116]. This was especially beneficial for oil recovery, as the low interfacial tension indicates that there are weaker forces that hold the liquid phases together [127,129]. According to Schramm et al (2003), a minimum interfacial tension at the oil/solution interface was found to have the maximum oil recovery efficiency. Furthermore, oil can easily encapsulate the microbubble at lower interfacial tension thus increasing attachment and therefore flotation of oil particles [13]. Therefore, the GNP addition could assist in the detachment of oil from contaminated sands, while improving the flotation of oil contaminants.

However, further increase in the GNP concentration above 0.1 wt% led to a gradual increment of interfacial tension. In accordance to **[121]**, this is due to the high concentrations of GNP which leads to the over-diffusion of graphene into the interface and the possible formation of a new graphene film dividing almost the whole interfacial area into a 3 phase layer with graphene in the middle of oil and water. The strength of this newly form graphene film is stronger than the initial film layer thus resulting to increase in interfacial tension.
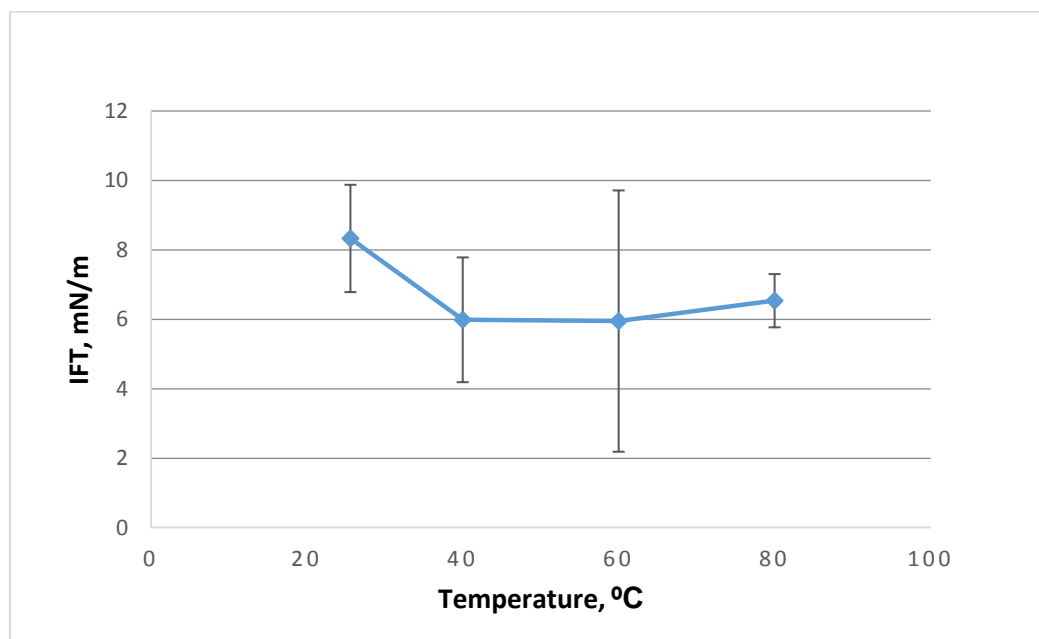
Figure 27 Interfacial tension against temperature

The interfacial tension against change in temperature at GNP concentration of 0.1 wt% is shown in **Figure 28**. It can be seen that the interfacial tension decreases as temperature increases. This is due to the weakening of molecular attractions between GNP particles and the fluid molecules as temperature increases thus resulting in a weaker interfacial strength **[118]**. Studies **[16,66,127]** have all indicated that interfacial lower interfacial tension was beneficial for oil recovery and was achieved with an increase in temperature. A study by Chou et al (1998), investigating the removal of non-volatile paraffin oil from contaminated soils via counter-current column flotation, found that an increase in temperature from 22 ^{o}C to 45 ^{o}C showed an increase in flotation efficiency from 62% to 78% which was attributed to the decrease molecule attraction and interfacial tension.

4.2.3 pH and viscosity measurements

The GNP dispersions were also characterised by viscosity and pH measurements. The effects of GNP concentration levels on pH and viscosity are summarized in **Figure 29**. It can be seen that the pH of water is inherently reduced with the addition of GNP, thus suggesting that graphene is acidic in nature. Nonetheless, there are no significant changes to pH levels and viscosity with the increase of GNP concentration in the solution. The lack of change in pH levels proves beneficial to soil remediation as it eliminates the need for chemical reduction of pH levels when graphene is supplemented.
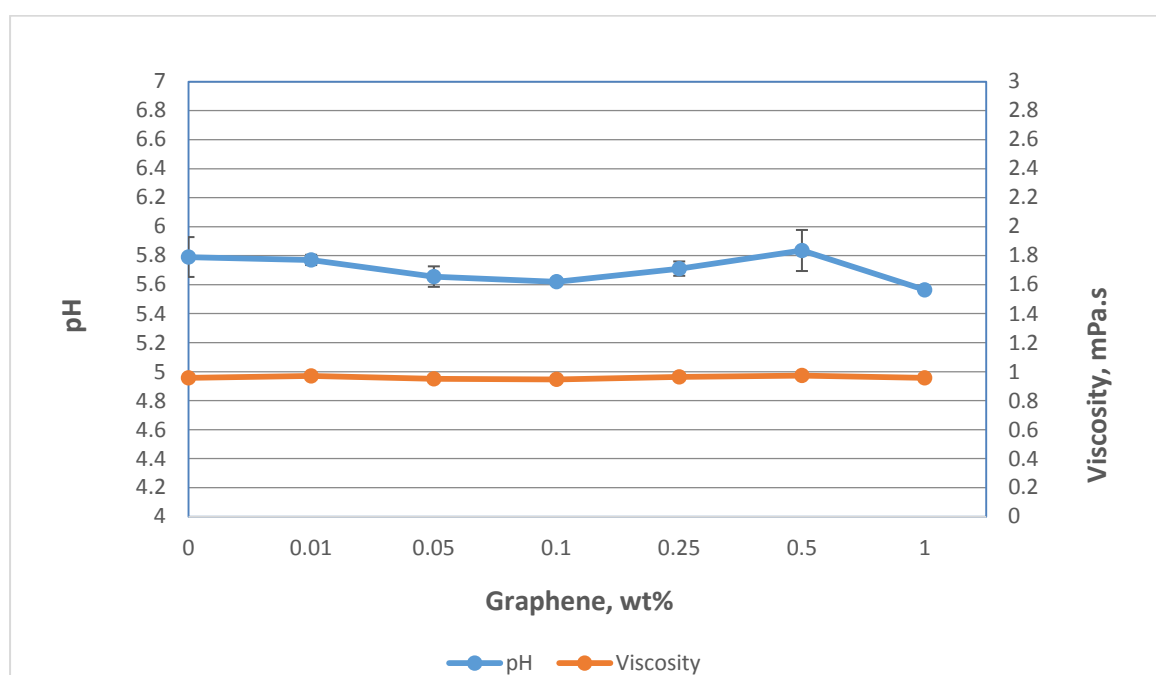
Figure 28 viscosity and pH against GNP concentration

The effects of temperature on pH levels and viscosity are also shown in **Figure 30.** Similarly, only small variations to the pH and viscosity were observed. From room temperature to 80 ℃, pH levels only increased from 5.58 to 5.89 while viscosity decreased by 0.3 mPa.s. The small change in viscosity is attributed to weakening of intermolecular bonds due to the increase of energy **[118]**. However, these changes are deemed too small to be significant and are considered to be negligible.
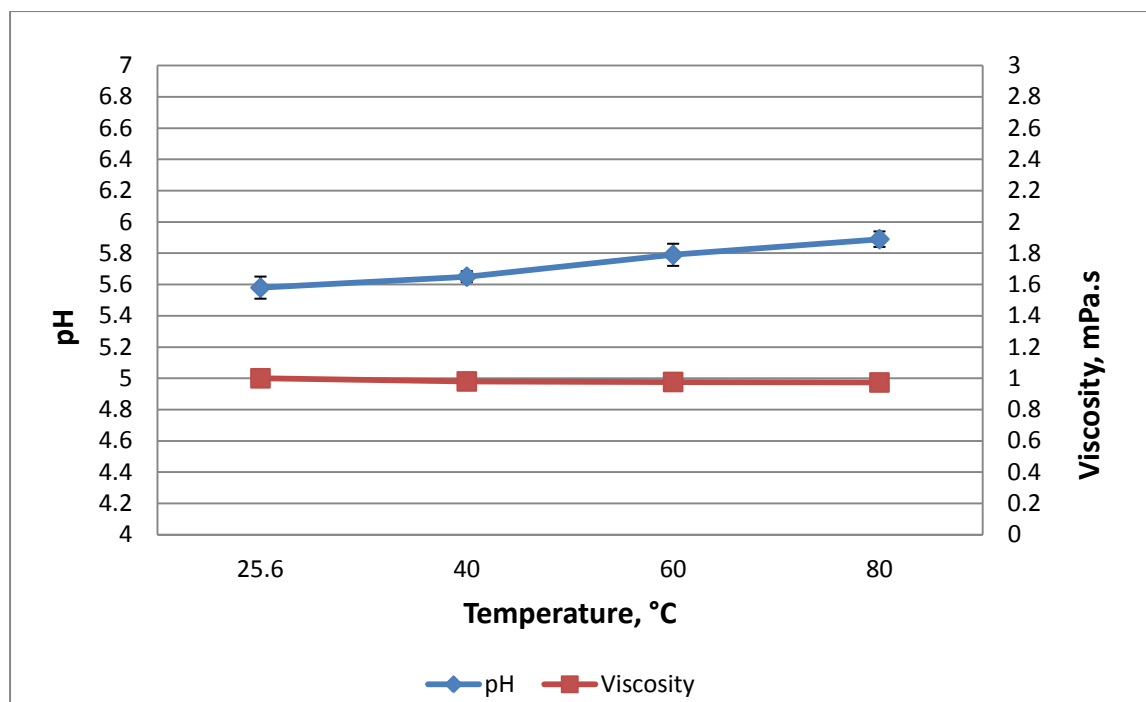
Figure 29 pH and viscosity against temperature

4.3 Graphene supplemented microbubble oil flotation efficiency

4.3.1 Oil recovery efficiency against GNP concentration

The effects of GNP concentration against oil recovery efficiency of graphene supplemented microbubbles oil flotation was conducted using the laboratory scale flotation setup. This was done to determine the optimum GNP concentration to achieve the highest recovery rate from oil contaminated soil at neutral pH.
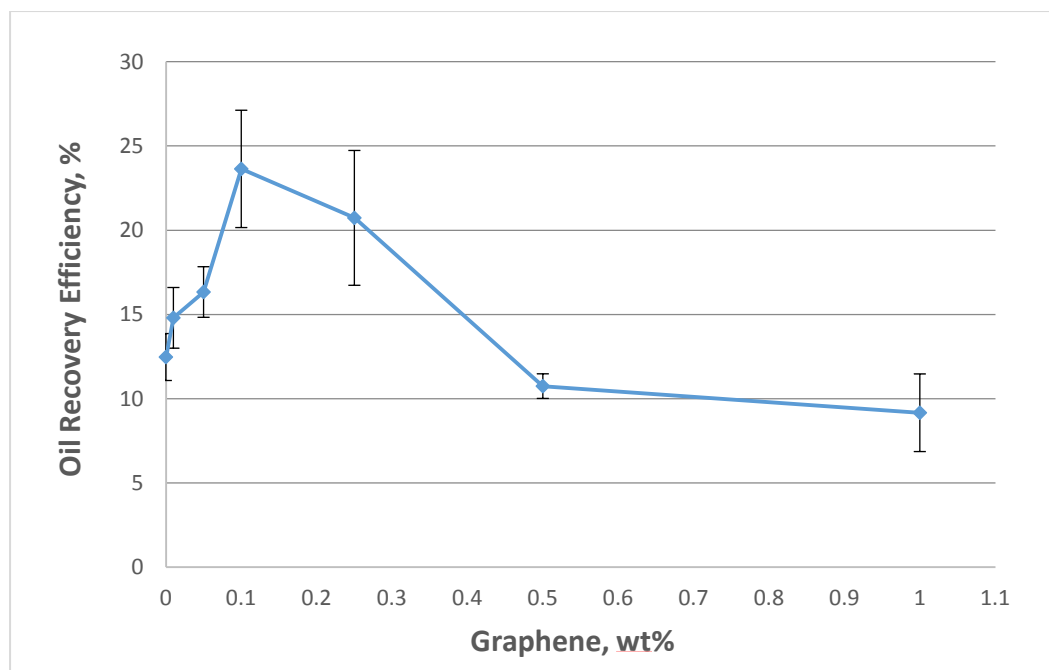
Figure 30 Oil recovery efficiency against GNP concentration

In **Figure 31,** the oil recovery efficiency increases until the concentration of GNP is at 0.1 wt% and starts to decrease as the concentration of graphene increases. At GNP concentration of 0.1 wt%, the oil recovery efficiency was at the maximum of 23.7%. At 0 wt% graphene concentration, where as a controlled study, the experiment was carried out complete graphene-free resulted in an oil recovery efficiency of 15%. This indicates a significant 10% increase in efficiency when graphene is supplemented at its optimum amount. From **4.2.2**, it determined that the addition of graphene causes a drop in interfacial tension (IFT) between water and crude oil and also attaching to microbubbles which starts to dislodge crude oil particles from the sand particles thus resulting in the increase in oil recovery efficiency **[118,121]**. However, when GNP is added over the optimum amount, the efficiency begins to decrease, to as low as 9%. This can be attributed to the saturation of graphene particles in the water mixture. The overloading of graphene particles attaching to a microbubble, increasing the weight carried and thus destabilizing the bubble as it ascends **[121]**. Also, as noted in **4.1.2**, it was noted that the over presence of graphene causes the formation of a new graphene film at the interface between crude oil and water which has a higher IFT thus becoming a hindrance towards removing the crude oil particles **[121]**. The trend oil

recovery rate against GNP concentration can be seen to display an inverse trend of the IFT against GNP concentration in **Figure 26.**

4.3.2 Oil recovery efficiency against pH
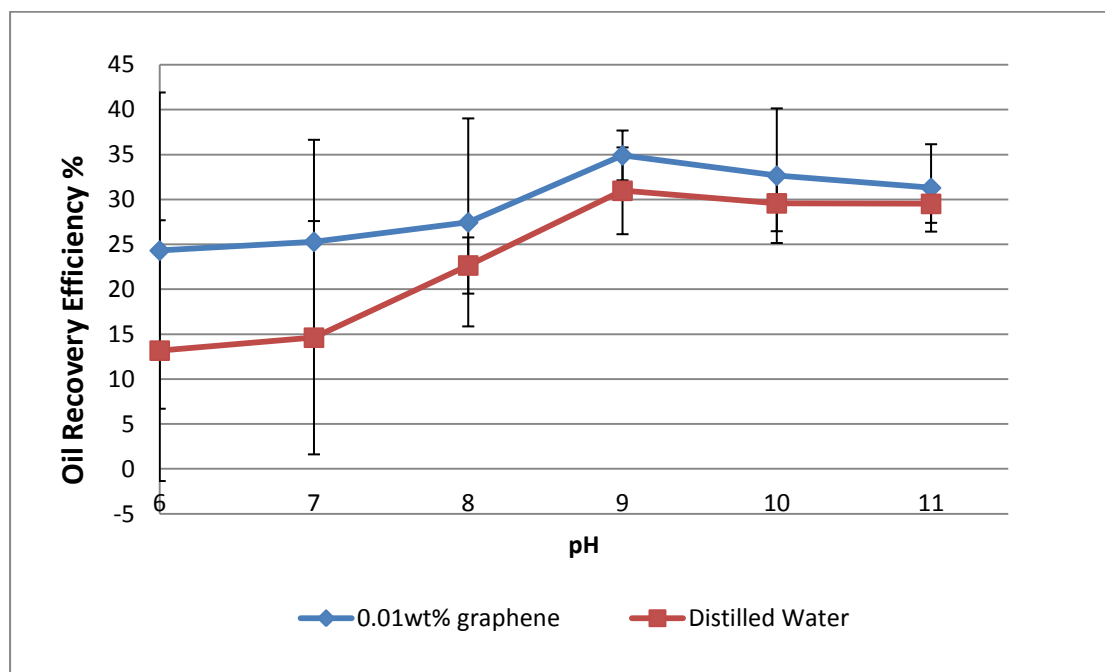
Figure 31 Oil recovery efficiency against pH for oil flotation with 0.1 wt% graphene and distiller water

Figure 32 indicates that the oil recovery efficiency of the flotation method with and without 0.1 wt% graphene against alkaline pH levels. At pH 6, graphene supplemented flotation has a recovery rate of 24.32 % while distilled water flotation has a recovery rate of 13.18 %. The graph indicates that both oil recovery efficiencies increase as pH levels increase until pH 9, with 0.01wt% graphene flotation at 34.92 % and distilled water flotation at 30.58 %. Under alkaline conditions, oil-sand bonds are weaker and thus separation becomes easier, therefore oil recovery increases **[127]**. Similar to **[125]**, as pH levels increase pass pH9, the oil recovery rate becomes constant, where oil-sand separation efficiency is at its maximum.
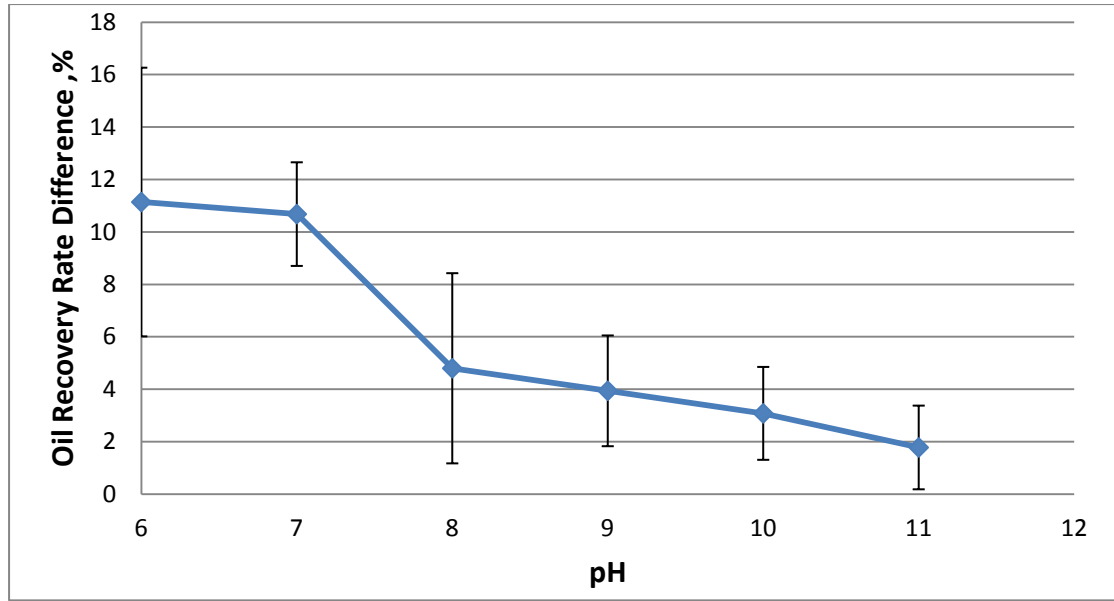
Figure 32 Difference in oil recovery efficiency of oil flotation with and without graphene against pH

The contributions of graphene to the oil recovery of the flotation method are displayed in the **Figure 33**. It can be seen that the difference in oil recovery decreases as pH levels increases. This indicates that the supplemented graphene becomes less effective as pH levels increase, which acts in accordance to **Figure 24** which indicates the total interparticle forces between graphene-microbubble increases with pH. Nonetheless, it was observed that oil recovery was still high at pH 9. This is largely contributed by the better separation/detachment of oil from sand due to alkaline conditions, as stated in **[125].** As previously determined in **4.1.4**, graphene-microbubble attachment becomes significantly more difficult as pH levels increase pass pH 9. This is displayed in **[125]**, where the efficiency with graphene begins to decrease pass pH9 while the efficiency without graphene remains constant.

Therefore, it is determined that the optimum pH level for graphene supplemented flotation is pH9. However, the supplemented graphene is most effective at a neutral pH level with an efficiency rate of 24.32 %. Hence, it is a better choice to use GNP at neutral pH levels as a substitute for increasing alkaline conditions.

4.3.3 Oil recovery efficiency against temperature
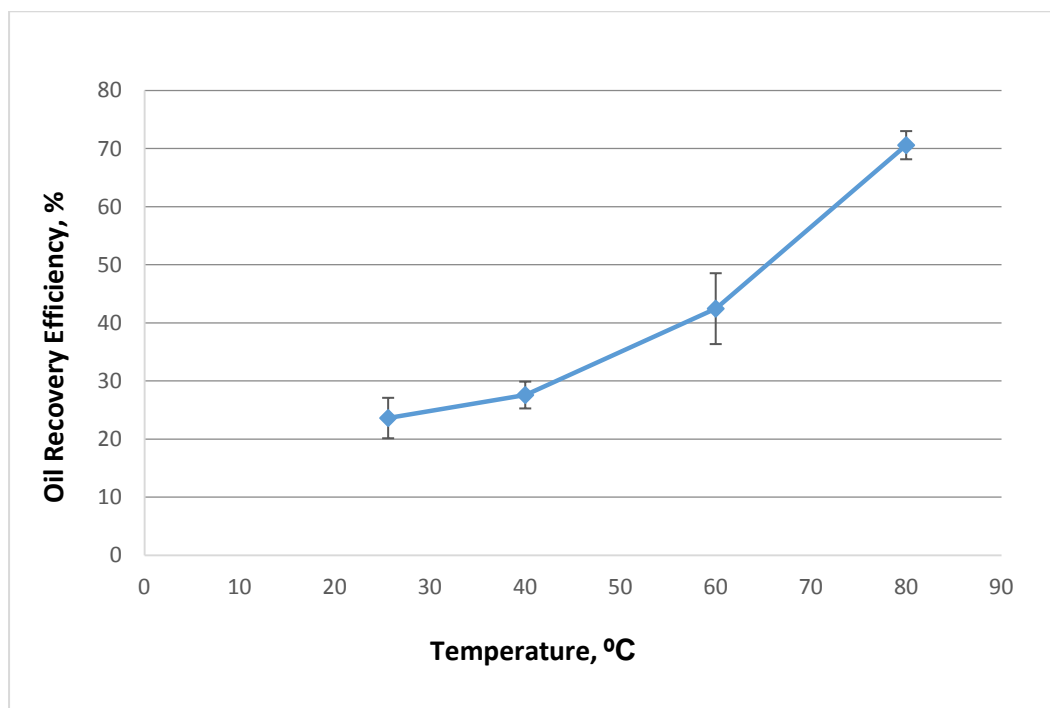
Figure 33 Oil recovery efficiency against temperature at 0.1 wt% GNP concentration

The effects of temperature against oil recovery efficiency of graphene supplemented microbubbles oil flotation was also conducted using the laboratory scale flotation setup. **Figure 34** displays the effects of temperature at the optimum GNP concentration of 0.1 wt% and neutral pH. From the results, it can be seen that the oil recovery rate increases as temperature increases. Oil removal efficiency of 70 % was achieved at 80 ℃ as compared to the 24 % at room temperature. This significant increase is attributed to the decrease in oil density as temperature increase **[130]**. This is shown in **Figure 35**.
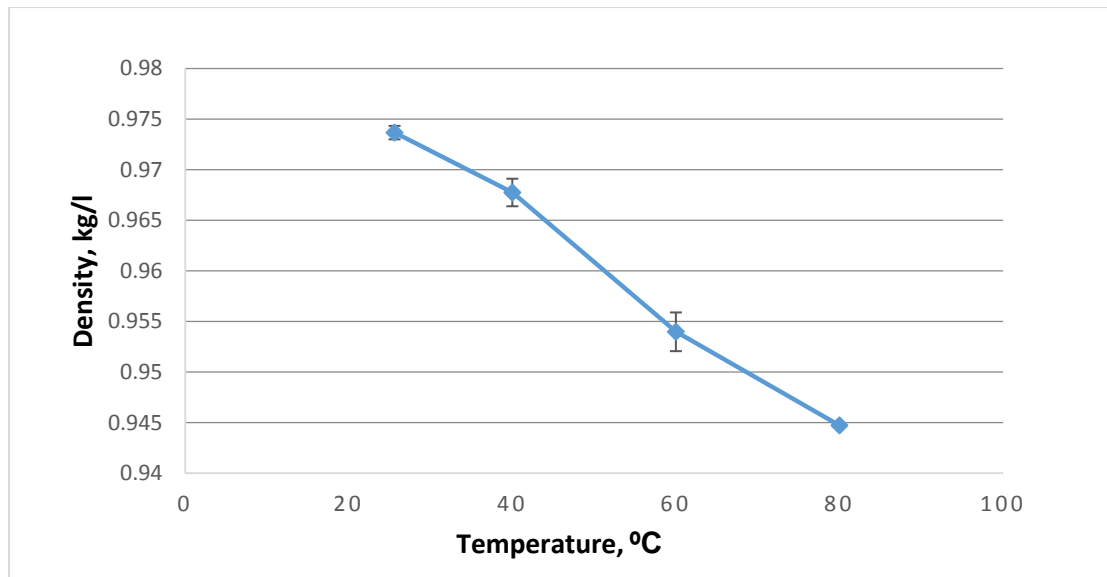
Figure 34 Oil density against temperature

The adhesive forces that hold the crude oil to sand particles become weaker as the temperature increases resulting in easier detachment of the oil particles [84]. Lower density equates to higher buoyancy forces thus crude oil particles with higher temperature are easier to float [125,130]. A change in density of crude oil will also affect the viscosity, as discussed in [131], where a decrease in density would result in a decrease of viscosity thus allowing for crude oil particles to float more easily. Furthermore, the adhesive forces of sand particles would also become weaker with increasing temperature thus resulting in higher oil-sand separation [125]. Overall, temperature is seen to play an important role in oil removal efficiency of the system.

4.3.4 Standard deviation of results for oil recovery rates

During the experiments to determine oil recovery rates of graphene supplemented microbubble flotation, the tests were repeated several times in order to obtain an accurate set of results.
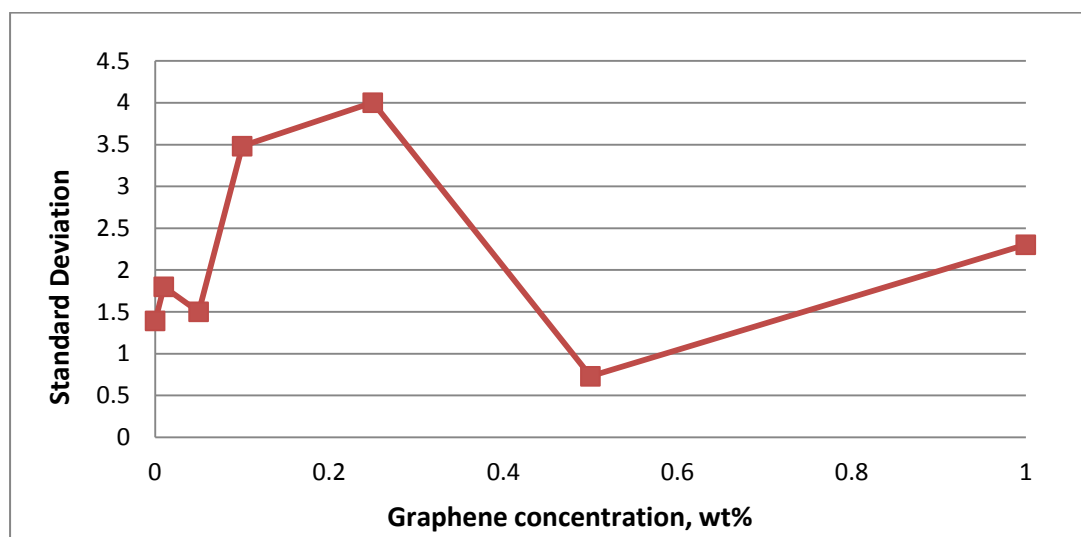
Figure 35 Standard deviation against graphene concentration

A maximum standard deviation of oil recovery rate of graphene supplemented microbubble flotation was displayed at ± 4.001 in **Figure 35**. This test was conducted 3 times and the fluctuations in the standard deviation would be attributed to the difficulty in obtaining an accurate measurement of graphene concentration.
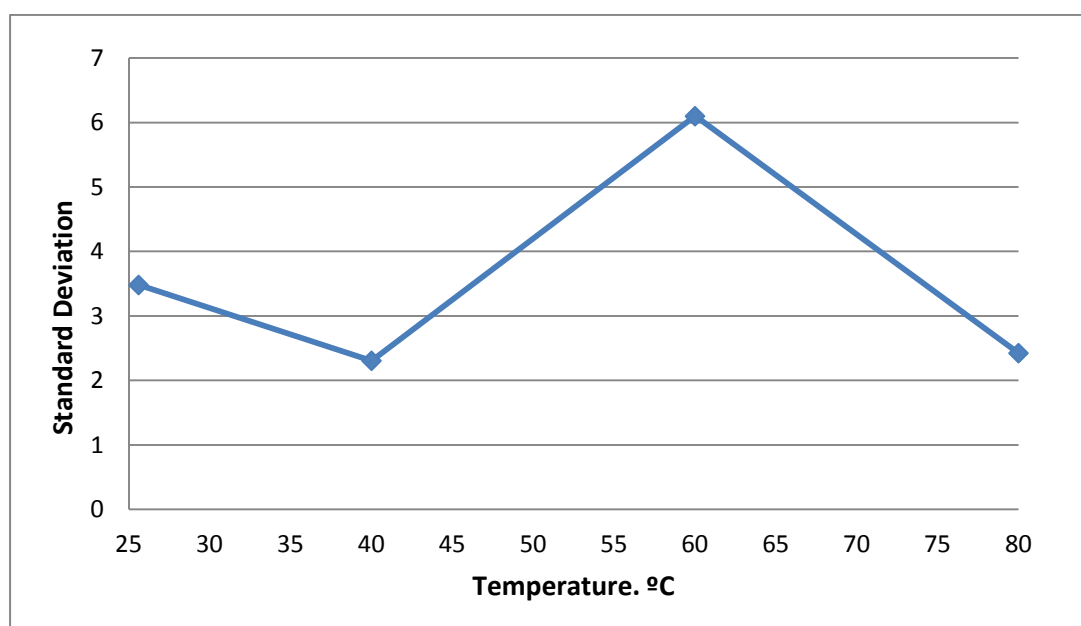
Figure 36 Standard deviation against temperature

During the oil recovery rate tests against temperature, discrepancies in the results obtained is due to the ability to maintain a constant temperature through the duration of the tests. Similarly, the tests were conducted 3 times to obtain accurate results. The standard deviation against temperature is displayed in **Figure 36** and it can be seen that the highest standard deviation was ± 6.1 thus indicating the effects of temperature control on the accuracy of this test.
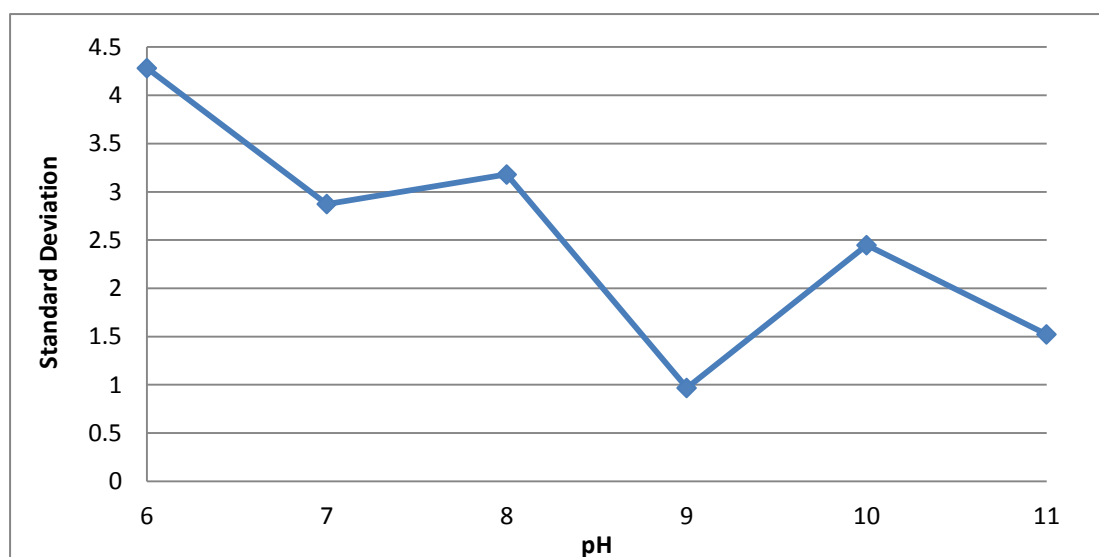
Figure 37 Standard deviation against pH

The oil recovery rate against pH levels were conducted 4 times due to the difficulty of achieving an accurate level of pH in the flotation column. It can be seen in **Figure 37** that the highest standard deviation measured was ± 4.282.

CHAPTER 5: CONCLUSIONS

5.1 Conclusions

The objective of this experiment was to determine the effects of supplementing graphene to the flotation oil recovery method and the effects of factors such as GNP pH levels, GNP concentration, and temperature on the oil recovery efficiency. Microbubble generation via venturi tube, for the effects of GNP concentration and temperature, and pH levels, was investigated in this experiment.

From previous literature, it was determined that oil/sand separation increases under alkaline conditions, and this research aimed to determine the effects of graphene added into the process. However, zeta potential measurements indicated that repulsion between graphene and microbubbles increases with pH levels thus the optimum pH for graphene-bubble attachment was at pH 7. An oil recovery rate of 24.32% was obtained. Therefore, it was concluded that the optimum pH for graphene supplemented microbubble oil flotation was at pH 7, albeit optimum oil-sand separation is higher under heavy alkaline conditions of pH 12 and above **[125]**. This was determined as the highest graphene-bubble attachment was found to be at neutral pH.

Next, the optimum GNP concentration was investigated to determine the highest oil recovery efficiency at pH 7. At GNP concentration of 0.1wt%, the oil recovery efficiency was at a maximum of 23.7%. Increasing GNP concentration further will result in lower oil recovery as the graphene particles will cause microbubbles to collapse due to overweighting before floating to the surface. Furthermore, over supply of graphene tend to form a thin layer in between oil and water thus becoming a hindrance to oil recovery. It was also determined that increase in temperature results in decrease of density and viscosity of oil hence an increase in oil recovery as it require less effort from the graphene/microbubbles to detach oil from sand. A maximum efficiency of 70% was obtained at 80˚C.

In conclusion, the addition of graphene provided an increase to the oil recovery rate from oil contaminated sand via the flotation method under specific conditions such as graphene concentration, temperature and pH level.

REFERENCES

[1]   M.W. Lim, E. V. Lau, and P. E. Poh, "A comprehensive guide of remediation technologies for oil contaminated soil — Present works and future directions" , *Marine Pollution Bulletin,* vol. 109, pp. 14-45, 2016.

[2]   P.J.V. Gupta, R. Gaur, M. Lowry, D. Jaroli and U. Chauhan, "Bioremediation of Petroleum oil Contaminated Soil and Water", *Research Journal of Environmental Toxicology,* vol. 5, pp. 1-26, 2011.

[3]   N. a. C. Das, P., "Microbial Degradation of Petroleum Hydrocarbon Contaminants: An Overview", *Biotechnology Research International,* pp. 1-13, 2011.

[4]   British Broadcasting Corporation News. (2010, May). Gulf of Mexico oil leak 'worst US environment distaster. [Online]. Viewed 2016 December 1. Available: https://www.bbc.co.uk/news/10194335

[5]   A. C. Bejarano and J. Michel, "Oil spills and their impacts on sand beach invertebrate communities: A literature review", *Environmental Pollution,* vol. 218, pp. 709-722, 2016.

[6]   A. C. Bejarano and J. Michel, "Oil spills and their impacts on sand beach invertebrate communities: A literature review", *Environmental Pollution,* vol. 218, pp. 709-722, 2016.

[7]   R. M. Abousnina, A. Manalo, W. Lokuge, and J. Shiau, "Oil Contaminated Sand: An Emerging and Sustainable Construction Material", *Procedia Engineering,* vol. 118, pp. 1119-1126, 2015.

[8]   A. Agarwal and Y. Liu, "Remediation technologies for oil-contaminated sediments", *Marine Pollution Bulletin,* vol. 101, pp. 483-490, 2015.

[9]   J. Hupka, J. D. Miller, and J. Drelich, "Water-Based Bitumen Recovery from Diluent-Conditioned Oil Sands", *The Canadian Journal of Chemical Engineering,* vol. 82, pp. 978-985, 2004.

[10]   J. Hupka and J. D. Miller, "Moderate-temperature water-based bitumen recovery from tar sand", *Fuel,* vol. 70, pp. 1308-1312, 1991.

[11]   L. L. Schramm and R. G. Smith, "The influence of natural surfactants on interfacial charges in the hot-water process for recovering bitumen from the athabasca oil sands", *Colloids and Surfaces,* vol. 14, pp. 67-85, 1985.

[12]   R. Pérez-Garibay, E. Martínez-Ramos, and J. Rubio, "Gas dispersion measurements in microbubble flotation systems", *Minerals Engineering,* vol. 26, pp. 34-40, 2012.

[13]   E. V. Lau, K. L. Foo, and P. E. Poh, "The Recovery of Oil from Oil/Sand Slurries in a Laboratory-Scale Flotation Cell", *IJESD,* pp. 351-354, 2013.

[14]   R. Pérez-Garibay, E. Martínez-Ramos, and J. Rubio, "Gas dispersion measurements in microbubble flotation systems", *Minerals Engineering,* vol. 26, pp. 34-40, 2012.

[15]   C.C. Chou, V. Ososkov, L. Zhang, P. Somasundaran, "Removal of nonvolatile hydrophobic compounds from artificially and naturally contaminated soils by column flotation", *Journal of Soil Contamination*, vol. 7, pp. 559 – 571, 1998.

[16]   L. Zhang, P. Somasundaran, V. Ososkov, C. Chou, "Flotation of hydrophobic contaminants from soil", *Colloids and Surfaces A: Physicochemical and Engineering Aspects*, vol. 177, pp. 235-246, 2000.

[17]   K. Urum, T. Pekdemir, M. Çopur, "Surfactants treatment of crude oil contaminated soils", *Journal of Colloid and Interface Science*, vol. 276, pp. 456-464, 2004.

[18]   A. M. Nazari, P. W. Cox, and K. E. Waters, "Copper ion removal from dilute solutions using ultrasonically synthesised BSA- and EWP-coated air bubbles", *Separation and Purification Technology*, vol. 132, pp. 218-225, 2014.

[19]   A. M. Nazari, P. W. Cox, and K. E. Waters, "Biosorption flotation of copper ions from dilute solution using BSA-coated bubbles", *Minerals Engineering*, vol. 75, pp. 140-145, 2015.

[20]   F. Zhou, L. Wang, Z. Xu, Q. Liu, and R. Chi, "Reactive oily bubble technology for flotation of apatite, dolomite and quartz", *International Journal of Mineral Processing*, vol. 134, pp. 74-81, 2015.

[21]   F. Zhou, L. Wang, Z. Xu, Q. Liu, and R. Chi, "Interaction of reactive oily bubble in flotation of bastnaesite", *Journal of Rare Earths*, vol. 32, pp. 772-778, 2014a.

[22]   American Physics Society (2009, October). This Month in Physics History, October 22, 2004: Discovery of Graphene. [Online]. Viewed 2016 December 1. Available: https://www.aps.org/publications/apsnews/200910/physics history.cfm

[23]   K. Lellala, K. Namratha, and K. Byrappa, "Ultrasonication assisted mild solvothermal synthesis and morphology study of few-layered graphene by colloidal suspensions of pristine graphene oxide", *Microporous and Mesoporous Materials,* vol. 226, pp. 522-529, 2016.

[24]   S. Yang, L. Chen, L. Mu, and P.C. Ma, "Magnetic graphene foam for efficient adsorption of oil and organic solvents", *Journal of Colloid and Interface Science,* vol. 430, pp. 337-344, 2014.

[25]   P.H. Chen, M.C. Sie, P.D. Jeng, R.C. Wu, and C.B. Wang, "Graphene sponge as an efficient and recyclable oil sorbent", *4th International Conference on the Advancement of Materials and Nanotechnology*, AIP Conference Proceedings 1877, pp. 030005-1 – 030005-10, 2017.

[26]   J.Y. Hong, E.H. Sohn, S. Park, and H.S. Park, Highly-efficient and recyclable oil absorbing performance of functionalized graphene aerogel", *Chemical Engineering Journal*, vol. 269, pp. 229-235, 2015.

[27]   D. Rushton, A.E. Ghaly, K. Martinell, "Assessment of Canadian regulations and remediation methods for diesel oil contaminated soils", *American Journal of Applied Sciences*, vol. 4, pp. 465-478, 2007.

[28]   M.T. Smith, F. Berruti, A.K. Mehrotra, "Thermal desorption treatment of contaminated soils in a novel batch thermal reactor", *Industrial & engineering chemistry research*, vol. 40, pp. 5421-5430, 2001.

[29]   A. Goi, M. Trapido, and N. Kulik, "Contaminated soil remediation with hydrogen peroxide oxidation", World Academy Science Engineering Technology, vol. 52, pp. 185-189, 2009.

[30]   R.Z. Hoff, "Bioremediation: an overview of its development and use for oil spill cleanup", *Marine Pollution Bulletin*, vol. 26, pp. 476-481, 1993.

[31]   S. Peng, Q. Zhou, Z. Cai,and Z. Zhang, "Phytoremediation of petroleum contaminated soils by Mirabilis Jalapa L. in a greenhouse plot experiment", *Journal of Hazardous Materials*, vol. 168, pp. 1490-1496, 2009.

[32]   N. Merkl, R. Schultze-Kraft, and M. Arias, "Influence of fertilizer levels on phytoremediation of crude oil-contaminated soils with the tropical pasture grass Brachiaria brizantha (Hochst. ex A. Rich.) Stapf", *International Journal of Phytoremediation*, vol. 7, pp. 217-230, 2005.

[33]   D. Tao, "Role of bubble size in flotation of coarse and fine particles—a review", *Separation science and technology*, vol.39, pp. 741-760,   2005.

[34]   J. Ralston, "Controlled flotation processes: Prediction and manipulation of bubble-particle capture", *The Journal of The South African Institute of Mining and Metallurgy*, vol. 99(1), pp. 27-34, 1999.

[35]   B. A. Wills and J. A. Finch, "Chapter 12 - Froth Flotation," in *Wills' Mineral Processing Technology (Eighth Edition)*, ed Boston: Butterworth-Heinemann, 2016, pp. 265-380.

[36]   J.K. Edzwald, "Principles and applications of dissolved air flotation", *Water Science and Technology*, vol. 31, pp.1-23, 1995.

[37]   A. Zouboulis, and A. Avranas, "Treatment of oil-in-water emulsions by coagulation and dissolved-air flotation", *Colloids and Surfaces A: Physicochemical and Engineering Aspects,* vol. 172, pp. 153-161, 2000.

[38]   H. Kiuri, "Development of dissolved air flotation technology from the first generationto the newest (third) one (DAF in turbulent flow conditions)", *Water Science & Technology*, vol. 43, pp. 1-7, 2001.

[39]   A. Al-Shamrani, A. James, and H. Xiao, "Destabilisation of oil–water emulsions and separation by dissolved air flotation", *Water Research*, vol. 36, pp. 1503-1512, 2002.

[40]   P.A. Hong, Z. Cha, X. Zhao, C.-J. Cheng, and W. Duyvesteyn, "Extraction of bitumen from oil sands with hot water and pressure cycles", *Fuel Processing Technology*, vol. 106, pp. 460-467, 2013.

[41]   Z. Zhou, R. Chow, P. Cleyle, Z. Xu, and J. Masliyah, "Effect of Dynamic Bubble Nucleation on Bitumen Flotation", *Canadian Metallurgical Quarterly*, vol. 49, pp. 363-372, 2010.

[42]   A. El-Kayar, M. Hussein, A. Zatout, A. Hosny, and A. Amer, "Removal of oil from stable oil-water emulsion by induced air flotation technique", *Separations Technology*, vol. 3, pp. 25-31, 1993.

[43]   N.J. Van Ham, L.A. Behie, and W.Y. Svrcek, "The effect of air distribution on the induced air flotation of fine oil in water emulsions", *The Canadian Journal of Chemical Engineering*, vol. 61, pp. 541-547, 1983.

[44]   G.J. Jameson, "Hydrophobicity and floc density in induced-air flotation for water treatment", *Colloids and Surfaces A: Physicochemical and engineering aspects*, vol. 151, pp. 269-281, 1999.

[45]   D. Deglon, "The effect of agitation on the flotation of platinum ores", *Minerals Engineering*, vol. 18, pp. 839-844, 2000.

[46]   P. Painmanakul, P. Sastaravet, S. Lersjintanakarn, and S. Khaodhiar, "Effect of bubble hydrodynamic and chemical dosage on treatment of oily wastewater by induced air flotation (IAF) process", *Chemical Engineering Research and Design*, vol. 88, pp. 693-702, 2010.

[47]   W. Sun, L. Ma, Y. Hu, Y. Dong, and G. Zhang, "Hydrogen bubble flotation of fine minerals containing calcium", *Mining Science and Technology (China)*, vol. 21, pp. 591-597, 2011.

[48]   A. Loh, and D.A. Israf, "Tests on the centrifugal flotation technique and its use in estimating the prevalence of Toxocara in soil samples from urban and suburban areas of Malaysia", *Journal of helminthology*, vol. 72, pp. 39-42, 1998.

[49]   M. Niewiadomski, A.V. Nguyen, J. Hupka, J. Nalaskowski, and J. Miller," Air bubble and oil droplet interactions in centrifugal fields during air-sparged hydrocyclone flotation", *International journal of environment and pollution*, vol. 30, pp. 313-331, 2007.

[50]   S. Watcharasing, W. Kongkowit, and S. Chavadej, "Motor oil removal from water by continuous froth flotation using extended surfactant: effects of air bubble parameters and surfactant concentration", *Separation and Purification Technology*, vol. 70, pp. 179-189, 2009.

[51]   A. Sobhy, and D. Tao, "Nanobubble column flotation of fine coal particles and associated fundamentals", *International Journal of Mineral Processing*, vol. 124, pp. 109-116, 2013.

[52]   A. Sobhy, and D. Tao, "High-Efficiency Nanobubble Coal Flotation", International *Journal of Coal Preparation and Utilization*, vol. 33, pp. 242-256, 2013.

[53]   J. Ran, J. Liu, C. Zhang, D. Wang, and X. Li, "Experimental investigation and modeling of flotation column for treatment of oily wastewater", *International Journal of Mining Science and Technology*, vol. 23, pp. 665-668, 2013.

[54]   T. Van Le, T. Imai, T. Higuchi, R. Doi, J. Teeka, S. Xiaofeng, and M. Teerakun, "Separation of oil-in-water emulsions by microbubble treatment and the effect of adding coagulant or cationic surfactant on removal efficiency", *Water Science & Technology*, vol. 66, pp. 1036-1043, 2012.

[55]   B. Li, D. Tao, Z. Ou, and J. Liu, "Cyclo-microbubble column flotation of fine coal", *Separation science and technology*, vol. 38, pp. 1125-1140, 2003.

[56]   X.B. Li, J.T. Liu, Y.T. Wang, C.Y. Wang, and X.H. Zhou, "Separation of oil from wastewater by column flotation", *Journal of China University of Mining and Technology*, vol. 17, pp. 546-577, 2007.

[57]   S. Vashisth, C.P. Bennington, J.R. Grace, and R.J. Kerekes, "Column Flotation Deinking: State-of-the-art and opportunities", *Resources, Conservation and Recycling*, vol. 55, pp. 1154-1177, 2011.

[58]   T. Napier-Munn, and B.A. Wills, "Wills' mineral processing technology: an introduction to the practical aspects of ore treatment and mineral recovery", Butterworth-Heinemann, 2011.

[59]   J. Rubio, M. Souza, and R. Smith, "Overview of flotation as a wastewater treatment technique", *Minerals Engineering*, vol. 15, pp. 139-155, 2002.

[60]   K. Clark, and D. Pasternack, "Hot water seperation of bitumen from Alberta bituminous sand", *Industrial & Engineering Chemistry*, vol. 24, pp. 1410-1416, 1932.

[61]   R. Martel, P.J. Gelinas, "Surfactant solution developed for NAPL recovery in contaminated aquifers", *Ground Water*, vol. 34(1), pp. 143-154, 1996.

[62]   D. H. Lee, R.D. Cody, D. J. Kim, and S. Choi, "Effect of soil texture on surfactant-based remediation of hydrophobic organic-contaminated soil", *Environmental International*, vol. 27, pp. 681-688, 2002.

[63]   M. Lee, H. Kang, and W. Do, "Application of nonionic surfactant-enhanced in situ flushing to a diesel contaminated site", *Water Research*, vol. 39, pp.139-146, 2005.

[64]   J.H. Harwell, D.A. Sabatini, and R.C. Knox, "Surfactants for groundwater remediation", *Colloids and Surfaces A:Physicochemical and Engineering Aspects*, vol. 151, pp. 255-268, 1999.

[65]   L. L. Schramm and R. G. Smith, "Two classes of anionic surfactants and their significance in hot water processing of oil sands", *The Canadian Journal of Chemical Engineering,* vol. 65, pp. 799-811, 1987.

[66]   L.L. Schramm, E.N. Stasiuk, D. Turner, "The influence of interfacial tension in the recovery of bitumen by water-based conditioning and flotation of Athabasca oil sands", *Fuel Processing Technology*, vol. 80, pp. 101-118, 2003.

[67]   C.W. Huang, and C.H. Chang, "A Laboratory Study on Foam-Enhanced Surfactant Solution Flooding in Removing n-Pentadecane from Contaminated Columns", *Colloids and Surfaces A:Physicochemical and Engineering Aspects*, vol. 173, pp. 171-179, 2000.

[68]   R.C.G. Oliveira, J.F. Oliveira, and B.M. Moudgil, "The effect of hydrophobic fine particles on the foam flushing remediation process", *Surface and Colloid Science*, vol. 128, pp. 293-297, 2004.

[69]   D. Roy, T.K. Valsaraj, and A. Tamoyo, "Comparation of soilwashing using conventional surfactant solutions and colloidal gas aphron suspension", *Separation Science and Technology*, vo. 27, pp. 1555-1568, 1992.

[70]   F.J. Brockman, W. Payne, D.J. Workman, A. Soong, S. Manley, and T.C. Hazen, "Effect of gasesous nitrogen and phosphorus injection on in situ bioremediation of a trichloroethylene-contaminated site", *Journal of Hazardous Materials*, vol. 41(2-3), pp. 287-298, 1995.

[71]   F. Sebba, " Microfoams—unexploited colloid system", *Colloid Interface Science*, vol. 35, pp. 643-646, 1971.

[72]   F. Sebba, "An improved generator for micron-sized bubbles", *Chemical Industry*, vol. 3, pp. 91-92,1987.

[73]   D. Roy, R.R. Kommalapati, K.T. Valsaraj, and W.D. Constant, "Soil flushing of residual transmission fluid: Application of Colloidal Gas Aphron suspensions and conventional surfactant solutions", *Water Research*, vol. 29(2), pp. 589-595, 1995.

[74]   H. J. B. Couto, G. Massarani, E. C. Biscaia Jr, and G. L. Sant'Anna Jr, "Remediation of sandy soils using surfactant solutions and foams", *Journal of Hazardous Materials,* vol. 164, pp. 1325-1334, 2009.

[75]   F. Lin, L. He, J. Hou, J. Masliyah, and Z. Xu, "Role of Ethyl Cellulose in Bitumen Extraction from Oil Sands Ores Using an Aqueous–Nonaqueous Hybrid Process", *Energy & Fuels,* vol. 30, pp. 121-129, 2016.

[76]   X. Ding, C. Repka, Z. Xu, and J. Masliyah, "Effect of Illite Clay and Divalent Cations on Bitumen Recovery", *The Canadian Journal of Chemical Engineering,* vol. 84, pp. 643-650, 2006.

[77]   S. Watcharasing, P. Angkathunyakul, and S. Chavadej, "Diesel oil removal from water by froth flotation under low interfacial tension and colloidal gas aphron conditions", *Separation and Purification Technology*, vol. 62, pp. 118-127, 2008.

[78]   J. Choi, E. Lee, S. Q. Choi, S. Lee, Y. Han, and H. Kim, "Arsenic removal from contaminated soils for recycling via oil agglomerate flotation", *Chemical Engineering Journal,* vol. 285, pp. 207-217, 2016.

[79]   L. L. Schramm, C. Morrison, and E. N. Stasiuk, "Some effects of chemical additions to nascent primary froth from the hot water flotation of bitumen from Athabasca oil sand", *Fuel Processing Technology,* vol. 56, pp. 243-261, 1998.

[80]   U. Farook, E. Stride, and M. Edirisinghe, "Stability of microbubbles prepared by co-axial electrohydrodynamic atomisation", *European Biophysics Journal,* vol. 38, pp. 713-718, 2009.

[81]   F. L. Tchuenbou-Magaia, and P. W. Cox, "TRIBOLOGICAL STUDY OF SUSPENSIONS OF CYSTEINE-RICH PROTEIN STABILIZED MICROBUBBLES AND SUBSEQUENT TRIPHASIC A/O/W EMULSIONS", *Journal of Texture Studies,* vol. 42, pp. 185-196, 2011.

[82]   H. Ikeura, F. Kobayashi, and M. Tamaki, "Removal of residual pesticide, fenitrothion, in vegetables by using ozone microbubbles generated by different methods", *Journal of Food Engineering,* vol. 103, pp. 345-349, 2011.

[83]   M. Ashokkumar, D. Sunartio, S. Kentish, R. Mawson, L. Simons, K. Vilkhu, and C.K. Versteeg, "Modification of food ingredients by ultrasound to improve functionality: a preliminary study on a model system", *Innovative Food Science & Emerging Technologies,* vol. 9, pp. 155-160, 2008.

[84]   S. Sirsi and M. Borden, "Microbubble compositions, properties and biomedical applications", *Bubble Science, Engineering & Technology,* vol. 1, pp. 3-17, 2009.

[85]   S. Hernot and A. L. Klibanov, "Microbubbles in ultrasound-triggered drug and gene delivery", *Advanced drug delivery reviews,* vol. 60, pp. 1153-1166, 2008.

[86]   J. G. Riess, "Blood substitutes and other potential biomedical applications of fluorinated colloids," *Journal of Fluorine Chemistry,* vol. 114, pp. 119-126, 2002.

[87]   E. C. Unger, T. Porter, W. Culp, R. Labell, T. Matsunaga, and R. Zutshi, "Therapeutic applications of lipid-coated microbubbles," *Advanced drug delivery reviews,* vol. 56, pp. 1291-1314, 2004.

[88]   K. Terasaka, A. Hirabayashi, T. Nishino, S. Fujioka, and D. Kobayashi, "Development of microbubble aerator for waste water treatment using aerobic activated sludge", *Chemical engineering science,* vol. 66, pp. 3172-3179, 2011.

[89] S. Liu, Q. Wang, H. Ma, P. Huang, J. Li, and T. Kikuchi, "Effect of micro-bubbles on coagulation flotation process of dyeing wastewater", *Separation and Purification Technology,* vol. 71, pp. 337-346, 2010.

[90] A. Al-Shamrani, A. James, and H. Xiao, "Separation of oil from water by dissolved air flotation", *Colloids and Surfaces A: Physicochemical and Engineering Aspects,* vol. 209, pp. 15-26, 2002.

[91] J. Hanotu, H. H. Bandulasena, T. Y. Chiu, and W. B. Zimmerman, "Oil emulsion separation with fluidic oscillator generated microbubbles", *International Journal of Multiphase Flow,* vol. 56, pp. 119-125, 2013.

[92] N. Ahmed and G.J. Jameson, "The Effect of Bubble Size on the Rate of Flotation of Fine Particles", *International Journal of Mineral Processing*, vol. 14(3), pp. 195-215, 1985.

[93] M. Kukizaki and M. Goto, "Spontaneous formation behavior of uniform-sized microbubbles from Shirasu porous glass (SPG) membranes in the absence of water-phase flow", *Colloids and Surfaces A: Physicochemical and Engineering Aspects,* vol. 296, pp. 174-181, 2007.

[94] M. Kukizaki and T. Nakashima, "Acid leaching process in the preparation of porous glass membranes from phase-separated glass in the Na2O-CaO-MgO-Al2O3-B2O3-SiO2 system", , vol. 29, pp. 301-308, 2004.

[95] M. Lee, E. Y. Lee, D. Lee, and B. J. Park, "Stabilization and fabrication of microbubbles: applications for medical purposes and functional materials", *Soft matter,* vol. 11, pp. 2067-2079, 2015.

[96] E. C. Unger, T. P. McCreery, R. H. Sweitzer, V. E. Caldwell, and Y. Wu, "Acoustically active liposheres containing paclitaxel: a new therapeutic ultrasound contrast agent", *Investigative radiology,* vol. 33, pp. 886-892, 1998.

[97] C. Christiansen, H. Kryvi, P. Sontum, and T. Skotland, "Physical and biochemical characterization of Albunex, a new ultrasound contrast agent consisting of air-filled albumin microspheres suspended in a solution of human albumin", *Biotechnology and applied biochemistry,* vol. 19, pp. 307-320, 1994.

[98] Y.-Z. Zhao, H.-D. Liang, X.-G. Mei, and M. Halliwell, "Preparation, characterization and in vivo observation of phospholipid-based gas-filled microbubbles containing hirudin", *Ultrasound in medicine & biology,* vol. 31, pp. 1237-1243, 2005.

[99]   P. Pattekari, Z.Zheng, X. Zhang, T.Levchenko, V. Torchilin, and Y.Lvov, "Top-down and bottom-up approaches in production of aqueous nanocolloids of low solubility drug paclitaxel", *Physical Chemistry Chemical Physics*, vol. 13(19), pp.9014-9019, 2011.

[100]   U. Farook, H. Zhang, M. Edirisinghe, E. Stride, and N. Saffari, "Preparation of microbubble suspensions by co-axial electrohydrodynamic atomization", *Medical engineering & physics,* vol. 29, pp. 749-754, 2007.

[101]   U. Farook, E. Stride, M. Edirisinghe, and R. Moaleji, "Microbubbling by co-axial electrohydrodynamic atomization", *Medical & biological engineering & computing,* vol. 45, pp. 781-789, 2007.

[102]   W. Teng, Z. Huneiti, W. Machowski, J. R. Evans, M. Edirisinghe, and W. Balachandran, "Towards particle-by-particle deposition of ceramics using electrostatic atomization", *Journal of materials science letters*, vol. 16, pp. 1017-1019, 1997.

[103]   E. Stride and M. Edirisinghe, "Novel microbubble preparation technologies," *Soft matter,* vol. 4, pp. 2350-2359, 2008.

[104]   Q. Xu and M. Nakajima, "The generation of highly monodisperse droplets through the breakup of hydrodynamically focused microthread in a microfluidic device", *Applied Physics Letters,* vol. 85, pp. 3726-3728, 2004.

[105]   K. Pancholi, U. Farook, R. Moaleji, E. Stride, and M. Edirisinghe, "Novel methods for preparing phospholipid coated microbubbles", *European Biophysics Journal,* vol. 37, pp. 515-520, 2008.

[106]   G. M. Whitesides, "The origins and the future of microfluidics", *Nature,* vol. 442, pp. 368-373, 2006.

[107]   S. L. Anna, N. Bontoux, and H. A. Stone, "Formation of dispersions using "flow focusing" in microchannels", *Applied physics letters,* vol. 82, pp. 364-366, 2003.

[108]   K. Hettiarachchi, E. Talu, M. L. Longo, P. A. Dayton, and A. P. Lee, "On-chip generation of microbubbles as a practical technology for manufacturing contrast agents for ultrasonic imaging", *Lab on a Chip,* vol. 7, pp. 463-468, 2007.

[109]   C. J. Harvey, J. M. Pilcher, R. J. Eckersley, M. J. Blomley, and D. O. Cosgrove, "Advances in ultrasound", *Clinical radiology,* vol. 57, pp. 157-177, 2002.

[110] N. C. Nanda, "History of echocardiographic contrast agents", *Clinical cardiology,* vol. 20, pp. 7-11, 1997.

[111] A. R. Jayaweera, N. Edwards, W. P. Glasheen, F. S. Villanueva, R. D. Abbott, and S. Kaul, "In vivo myocardial kinetics of air-filled albumin microbubbles during myocardial contrast echocardiography. Comparison with radiolabeled red blood cells", *Circulation Research,* vol. 74, pp. 1157-1165, 1994.

[112] R. Gramiak and P. M. Shah, "Echocardiography of the aortic root", *Investigative radiology,* vol. 3, pp. 356-366, 1968.

[113] A. K. Geim and K. S. Novoselov, "The rise of graphene", *Nature materials,* vol. 6, pp. 183-191, 2007.

[114] L.J. Cote, V.C. Tung, J. Luo, F. Kim, and J. Huang, "Graphene oxide as surfactant sheets", *Pure Appl. Chem,* vol. 83, pp. 95-110, 2010.

[115] H. Bi, X. Xie, K. Yin, Y. Zhou, S. Wan, L. He, F. Xu, F. Banhart, L. Sun, and R.S. Ruoff, "Spongy Graphene as a Highly Efficient and Recyclable Sorbent for Oils and Organic Solvents", *Advanced Functional Materials,* vol. 22, pp. 4421-4425, 2012.

[116] K. Y. Yoon, S. J. An, Y. Chen, J. H. Lee, S. L. Bryant, R. S. Ruoff*, et al.*, "Graphene oxide nanoplatelet dispersions in concentrated NaCl and stabilization of oil/water emulsions," *Journal of Colloid and Interface Science,* vol. 403, pp. 1-6, 2013.

[117] Y. He, Y. Liu, T. Wu, J. Ma, X. Wang, Q. Gong*, et al.*, "An environmentally friendly method for the fabrication of reduced graphene oxide foam with a super oil absorption capacity," *Journal of Hazardous Materials,* vol. 260, pp. 796-805, 2013.

[118] N. Ahammed, L. G. Asirvatham, and S. Wongwises, "Effect of volume concentration and temperature on viscosity and surface tension of graphene–water nanofluid for heat transfer applications," *Journal of Thermal Analysis and Calorimetry,* vol. 123, pp. 1399-1409, 2016.

[119] S. Yang, L. Chen, L. Mu, and P. C. Ma, "Magnetic graphene foam for efficient adsorption of oil and organic solvents," *J Colloid Interface Sci,* vol. 430, pp. 337-44, 2014.

[120] S. Kabiri, D. N. H. Tran, T. Altalhi, and D. Losic, "Outstanding adsorption performance of graphene–carbon nanotube aerogels for continuous oil removal," *Carbon,* vol. 80, pp. 523-533, 2014.

[121] S. Fang, T. Chen, R. Wang, Y. Xiong, B. Chen, and M. Duan, "Assembly of Graphene Oxide at the Crude Oil/Water Interface: A New Approach to Efficient Demulsification," *Energy & Fuels,* vol. 30, pp. 3355-3364, 2016.

[122] D. Luo, F. Wang, J. Zhu, F. Cao, Y. Liu, X. Li*, et al.*, "Nanofluid of graphene-based amphiphilic Janus nanosheets for tertiary or enhanced oil recovery: High performance at low concentration," *Proceedings of the National Academy of Sciences of the United States of America,* vol. 113, p. 7711, 2016.

[123] R. Greenwood, K. Kendall, "Electroacoustic studies of moderately concentrated colloidal suspensions", *Journal of European Ceramic Society*, vol. 19(4), pp.479-488,1999.

[124] D.A.H. Hanaor, M. Michelazzi, C. Leonilli, C.C. Sorrell, "The effects of carboxylic acids on the aqueous dispersion and electrophoretic deposition of ZrO_2", *Journal of the European Ceramic Society,* vol.32(1), pp.235-244,2012.

[125] M.W. Lim, E.V. Lau, P. Poh, and W. Chong, "Interaction studies between high-density oil and sand particles in oil flotation technology", *Journal of Petroleum Science and Engineering,* vol. 131, pp. 114-121, 2015.

[126] E.V. Lau, K.L. Foo and P.E. Poh, "The recovery of oil from oil/sand slurries in a laboratory-scale flotation cell", *International Journal of Environmental Science and Development*, vol. 4(4), pp. 352-354, 2013.

[127] Q. Dai and K.H. Chung, "Bitumen-sand interaction in oil sand processing", *Fuel*, vol.74 (12), 1858-1864, 1995.

[128] M.W. Lim, E.V. Lau, and P.E. Poh, "Optimization of Nanobubble-Assisted Bunker Oil Flotation from Oil-Wet Sand via Response Surface Methodology (RSM)", *ASEAN Journal of Chemical Engineering*, vol. 15, pp. 1-9, 2015.

[129] M.W. Lim, E.V. Lau, and P.E. Poh, "Analysis of attachment process of bubbles to high-density oil: Influence of bubble size and water chemistry", *Journal of the Taiwan Institute of Chemical Engineers*, vol. 68, pp. 192-200, 2016.

[130] L. L. Schramm, E. N. Stasiuk, H. Yarranton, B. B. Maini, and B. Shelfantook, "Temperature Effects From the Conditioning and Flotation of Bitumen From Oil Sands in Terms of Oil Recovery and Physical Properties", *Journal of Canadian Petroleum* Technology, vol. 42(8), pp. 55-61, 2003.

[131]   O. Alomair, A. Elsharkawy, and H. Alkandari, "A viscosity prediction model for Kuwaiti heavy crude oils at elevated temperatures", *Journal of Petroleum Science and Engineering*, vol. 120, pp. 102-110, 2014.

[132]   R. Pazhianur, and R. –H. Yoon, "Model for the origin of hydrophobic force", *Minerals and Metallurgical Processing*, vol. 20 (4), pp. 178 – 184, 2003.

[133]   L. Bergström, "Hamaker constants of inorganic materials", *Advances in Colloid and Interface Science*, vol. 70, pp. 125-169, 1997.

[134]   I. U. Vakarelski, R. Manica, X. Tang, S. J. O'Shea, G. W. Stevens, F. Grieser, R. R. Dagastine, and D. Y. C. Chan, "Dynamic interactions between microbubbles in water", *Proceedings of the National Academy of Sciences of the United States of America*, vol. 107 (25), 11177-11182, 2010.

[135]   DLVO Theory, Module 8: "Stability of Colloids" Lecture Notes. India: NPTEL, 2012.Viewed 2016 August 3. Available: https://nptel.ac.in/courses/103104045/pdf_version/lecture37.pdf

APPENDIX

Appendix A: Characterization Studies

Appendix A.1 Density measurement

Density vs Graphene concentraion

graphene wt%	trial 1	trial 2	trial 3	trial 4	AVERAGE	STDEV
0.01	0.991	0.9911	0.9916	0.9916	0.9913	0.00032
0.05	0.9916	0.9914	0.9913	0.9917	0.9915	0.000183
0.1	0.9918	0.9922	0.9922	0.9921	0.992075	0.000189
0.25	0.9925	0.9923	0.9928	0.993	0.99265	0.000311
0.5	0.9927	0.9916	0.9931	0.9934	0.9927	0.000787
1	0.9928	0.9924	0.9931	0.9932	0.992875	0.000359

Density vs Temperature

Temperature °C	trial 1	trial 2	trial 3	trial 4	AVERAGE	STDEV
25.6	0.9918	0.9922	0.9922	0.9921	0.992075	0.000189
40	0.9885	0.9898	0.9893	0.9892	0.9892	0.000535
60	0.9787	0.9817	0.9805	0.983	0.980975	0.001828
80	0.9776	0.9789	0.9809	0.9802	0.9794	0.001458

Oil density vs Temperature

Temperature	trial 1	trial 2	trial 3	trial 4	AVERAGE	STDEV
25.6	0.9735	0.9744	0.9731	0.9736	0.97365	0.000545
40	0.9694	0.9683	0.9669	0.9664	0.96775	0.001363
60	0.9537	0.953	0.9508	0.9556	0.953275	0.001982
80	0.9449	0.9447	0.9447	0.9446	0.944725	0.000126

Appendix A.2 Interfacial Tension Measurement

IFT vs grapheme concentratin

graphene wt%	trial 1	trial 2	trial 3	trial 4	AVERAGE	STDEV
0.01	20.82	15.83	19.11	18.59	18.5875	2.070497
0.05	12.1	11.32	10.69	10.59	11.175	0.696204
0.1	6.87	8.43	8.39	9.85	8.385	1.217032
0.25	4.88	10.45	10.11	13.55	9.7475	3.595204
0.5	32.88	19.94	10.05	15.19	19.515	9.782564
1	8.61	10.67	10.39	15.33	11.25	2.868914

IFT vs Temperature

Temperature	trial 1	trial 2	trial 3	trial 4	AVERAGE	STDEV
25.6	6.87	8.43	8.39	9.85	8.385	1.217032
40	**7.3**	**2.93**	**5.55**	**5.12**	5.225	1.797155
60	**7.27**	**3.47**	**12.61**	**7.12**	7.6175	3.763645
80	5.74	7.27	6.54	6.6	6.5375	0.626225

Appendix A.3 Viscosity Measurements

Viscosity vs grapheme concentration

graphene wt%	trial 1	trial 2	trial 3	trial 4	AVERAGE	STDEV
0.01	0.98	0.97	0.96	0.97	0.97	0.008165
0.05	0.95	0.95	0.93	0.96	0.9475	0.012583
0.1	0.95	0.94	0.95	0.95	0.9475	0.005
0.25	0.97	0.95	0.97	0.963	0.96325	0.00943
0.5	0.98	0.97	0.97	0.97	0.9725	0.005
1	0.97	0.95	0.95	0.97	0.96	0.011547

Viscosity vs Temperature

Temperature	trial 1	trial 2	trial 3	AVERAGE	STDEV
25.6	1.02	1	1	1.007	0.011547
40	1	1	1	1	0
60	0.98	0.98	0.97	0.976667	0.005774
80	0.97	0.98	0.97	0.973333	0.005774

Appendix A.4 pH measurements

Graphene concentration vs pH

Graphene concentration	pH'
0.01wt% graphene	5.7
0.05wt% graphene	5.65
0.1wt% graphene	5.62
0.25wt% graphene	5.71
0.5wt% graphene	5.84
1wt% graphene	5.64

Temperature of GNP solution vs pH

Temp	pH'
T = 25.6	5.58
T = 40	5.65
T = 60	5.79
T = 80	5.89

Appendix B: Graphene supplemented microbubble oil recovery flotation method

Appendix B1 Graphene concentration vs Oil recovery rate

Graphene wt%	Test 1	Test 2	Test 3	Avg	STDEV
0	11.2	12.26	13.96	12.47333	1.392312
0.01	16.6	13	14.8	14.8	1.8
0.05	14.8	17.8	16.4	16.33333	1.501111
0.1	25.7	25.6	19.62	23.64	3.481781
0.25	20.6	24.8	16.8	20.73333	4.001666
0.5	11.36	9.94	10.942	10.74733	0.729741
1	11.4	9.3	6.8	9.166667	2.302897

Appendix B2 Temperature vs Oil recovery rate

Temperature	Test 1	Test 2	Test 3	Avg	STDEV
25.6	25.7	25.6	19.62	23.64	3.481781
40	27.8	25.2	29.8	27.6	2.306513
60	48.6	42.4	36.4	42.46667	6.100273
80	73.2	68.4	70.2	70.6	2.424871

Appendix C: Analysis of zeta potential measurements

Appendix C1 Zeta potential measurement of graphene vs pH

ZETA	AVG ZETA	STDEV	PH	AVG PH
-30			6.1	
-30.2			6.12	
-31.7	-30.6333	0.929157	6.15	6.123333
-30.8			7.05	
-23.7			7.07	
-32.4	-28.9667	4.630695	7.1	7.073333
-33.1			8.11	
-38.5			8.21	
-37.9	-36.5	2.95973	8.19	8.17
-38.3			9.09	
-40.3			9.1	
-38.7	-39.1	1.058301	8.99	9.06
-49.2			9.9	
-46.9			9.88	
-51.3	-49.1333	2.200757	9.86	9.88
-60.4			10.82	
-64.2			10.97	
-66.7	-63.7667	3.172276	10.91	10.9

Appendix C2 Zeta potential measurements of microbubble vs pH

ZP	pH	Avg ZP	STDEV	Avg PH
-33.1	6.13			
-29.7	6.15			
-39.1	6.18	-33.9667	4.759552	6.153333
-31.5	7.18			
-34.2	7.24			
-37.8	7.3	-34.5	3.160696	7.24
-41.9	8.09			
-30.8	8.18			
-37.3	8.27	-36.6667	5.577036	8.18
-34.5	8.99			
-35.2	8.97			
-41.9	8.94	-37.2	4.08534	8.966667
-47	9.92			
-54.8	9.91			
-54.7	9.89	-52.1667	4.474744	9.906667
-56.2	10.9			
-63.3	10.9			
-62.2	10.9	-60.5667	3.821431	10.9

Appendix C2 Zeta potential measurements of oil droplets vs pH

ZETA	AVG ZETA	STDEV	PH	AVG PH
-19.389			6.1	
-22.984			5.8	
-23.039	-21.804	2.091632	5.97	5.956667
-30.8			7.01	
-23.7	-		7.07	
-32.4	28.9667	4.630695	6.99	7.023333
-35.1			8.11	
-39.5			8.01	
-37.9	-37.5	2.227106	7.919	8.013
-45.32			9.09	
-43.15	-		9.1	
-47.69	45.3867	2.270734	9.14	9.11
-53.3			10.23	
-57.43	-		10.34	
-55.45	55.3933	2.065583	9.8	10.12333
-64.4			10.82	
-72.2			10.97	
-70.7	-69.1	4.13884	10.91	10.9

Appendix C3 DVLO Theory

Total Force (pH)		pH					
Separation distance (H), nm	Separation distance (H), m	6	7	8	9	10	11
0.01	1E-11	-0.0003	-0.00098	0.000153	5.58E-05	0.000116	0.000376
0.05	5E-11	0.000153	1.18E-05	0.000295	0.000297	0.000509	0.000794
0.1	1E-10	0.000192	0.000119	0.000295	0.000309	0.000536	0.00082
0.2	2E-10	0.000205	0.000166	0.000286	0.000305	0.000534	0.000811
0.3	3E-10	0.000204	0.000176	0.000277	0.000298	0.000522	0.00079
0.4	4E-10	0.000201	0.000179	0.000268	0.000289	0.000507	0.000767
0.5	5E-10	0.000196	0.000177	0.00026	0.00028	0.000492	0.000744
0.6	6E-10	0.00019	0.000174	0.000251	0.000271	0.000477	0.00072
0.7	7E-10	0.000185	0.000171	0.000243	0.000263	0.000462	0.000698
0.8	8E-10	0.00018	0.000167	0.000235	0.000254	0.000448	0.000676
0.9	9E-10	0.000174	0.000162	0.000227	0.000246	0.000433	0.000654
1	0.000000001	0.000169	0.000158	0.00022	0.000238	0.00042	0.000633
2	0.000000002	0.000122	0.000116	0.000158	0.000172	0.000303	0.000456
3	0.000000003	8.82E-05	8.42E-05	0.000114	0.000124	0.000218	0.000328
4	0.000000004	6.35E-05	6.07E-05	8.18E-05	8.89E-05	0.000157	0.000236
5	0.000000005	4.57E-05	4.38E-05	5.88E-05	6.39E-05	0.000113	0.00017
6	0.000000006	3.28E-05	3.15E-05	4.23E-05	4.59E-05	8.09E-05	0.000122
7	0.000000007	2.36E-05	2.27E-05	3.04E-05	3.3E-05	5.82E-05	8.77E-05
8	0.000000008	1.7E-05	1.63E-05	2.19E-05	2.37E-05	4.18E-05	6.3E-05
9	0.000000009	0.000	1.17E-05	1.57E-05	1.71E-05	3.01E-05	4.53E-05
10	0.00000001	8.78E-06	8.43E-06	1.13E-05	1.23E-05	2.16E-05	3.26E-05

Appendix D: Oil removal efficiency vs pH

Appendix D1 Oil Recovery rate with graphene vs pH

ph	test 1 (%)	test 2 (%)	test 3 (%)	test 4 (%)	test 5 (%)	Average (%)	STDEV
6	27.4	21.6	29.3	24.6	18.7	24.32	4.282172
7	29.4	23.4	22.7	27.2	23.8	25.3	2.874022
8	23	26.8	27.5	28.1	31.9	27.46	3.180094
9	34.6	35.6	34.9	36	33.5	34.92	0.967988
10	34.6	34	32.5	33.7	28.5	32.66	2.44806
11	29.4	30.2	31.4	32.4	33.1	31.3	1.523155

Appendix D2 Oil Recovery rate with distilled water vs pH

ph	test 1 (%)	test 2 (%)	test 3 (%)	test 4 (%)	test 5 (%)	Average (%)	STDEV
6	15.4	14.2	11.6	10.8	13.9	13.18	1.913635
7	17	11.7	14.5	15	14.9	14.62	1.89921
8	22.7	23	22.7	23.4	21.5	22.66	0.709225
9	33.4	30.8	29.8	29.7	31.2	30.98	1.497331
10	30.4	30.6	29.4	29.1	28.4	29.58	0.917606
11	30.1	28.6	29.4	30.1	29.4	29.52	0.622093